NAVAL POSTGRADUATE SCHOOL
Monterey, California

THESIS

NATURAL CONVECTION IMMERSION COOLING
OF AN ARRAY OF SIMULATED CHIPS
IN AN ENCLOSURE FILLED WITH DIELECTRIC
LIQUID

by

Turgay Pamuk

December 1987

Thesis Advisor M.D. Kelleher
Co-Advisor Yogendra Joshi

Approved for public release; distribution is unlimited.

SECURITY CLASSIFICATION OF THIS PAGE

REPORT DOCUMENTATION PAGE

1a REPORT SECURITY CLASSIFICATION UNCLASSIFIED	1b RESTRICTIVE MARKINGS
2a SECURITY CLASSIFICATION AUTHORITY	3 DISTRIBUTION/AVAILABILITY OF REPORT Approved for public release; distribution is unlimited
2b DECLASSIFICATION/DOWNGRADING SCHEDULE	
4 PERFORMING ORGANIZATION REPORT NUMBER(S)	5 MONITORING ORGANIZATION REPORT NUMBER(S)
6a NAME OF PERFORMING ORGANIZATION Naval Postgraduate School 6b OFFICE SYMBOL (If applicable) 69	7a NAME OF MONITORING ORGANIZATION Naval Postgraduate School
6c ADDRESS (City, State, and ZIP Code) Monterey, California 93943-5100	7b ADDRESS (City, State, and ZIP Code) Monterey, California 93943-5100
8a NAME OF FUNDING/SPONSORING ORGANIZATION 8b OFFICE SYMBOL (If applicable)	9 PROCUREMENT INSTRUMENT IDENTIFICATION NUMBER
8c ADDRESS (City, State, and ZIP Code)	10 SOURCE OF FUNDING NUMBERS PROGRAM ELEMENT NO / PROJECT NO / TASK NO / WORK UNIT ACCESSION NO

11 TITLE (Include Security Classification)
Natural convection immersion cooling of an array of simulated chips in an enclosure filled with dielectric liquid

12 PERSONAL AUTHOR(S) Pamuk, Turgay

13a TYPE OF REPORT	13b TIME COVERED	14 DATE OF REPORT (Year Month Day)	15 PAGE COUNT
Masters/Eng thesis	FROM _____ TO _____	1987 December	71

16 SUPPLEMENTARY NOTATION

17 COSATI CODES			18 SUBJECT TERMS (Continue on reverse if necessary and identify by block number)
FIELD	GROUP	SUB-GROUP	Natural convection, free convection, cubical or rectangular enclosures, electronic cooling

19 ABSTRACT (Continue on reverse if necessary and identify by block number)

An experimental natural convection heat transfer study of a simulated electronic circuit board has been conducted. The board has an array of 9 simulated chips , each dissipating up to 2.5 Watts. The board is immersed in FC75, a fluorocarbon liquid, in an enclosure whose top and bottom surfaces are constant temperature heat sinks. The experimental data have been expressed in terms of relevant dimensionless heat transfer parameters such as Nusselt and Rayleigh numbers. The trend is that, the chips located higher in the enclosure have lower heat transfer rates. Otherwise the chips in the same row behave in a similar way which implies a quasi-two dimensionality.

20 DISTRIBUTION/AVAILABILITY OF ABSTRACT ☒ UNCLASSIFIED/UNLIMITED ☐ SAME AS RPT ☐ DTIC USERS	21 ABSTRACT SECURITY CLASSIFICATION UNCLASSIFIED
22a NAME OF RESPONSIBLE INDIVIDUAL T. D. KELLEHER	22b TELEPHONE (Include Area Code) 646-2530 22c OFFICE SYMBOL 69Kk

DD FORM 1473, 84 MAR 83 APR edition may be used until exhausted
All other editions are obsolete

SECURITY CLASSIFICATION OF THIS PAGE
UNCLASSIFIED

☆ U.S. Government Printing Office 1986—606-24

Approved for public release; distribution is unlimited.

Natural Convection Immersion Cooling of an Array of Simulated Chips in an Enclosure Filled With Dielectric Liquid

by

Turgay Pamuk
Lieutenant Junior Grade, Turkish Navy
B.S., Turkish Naval Academy, 1981

Submitted in partial fulfillment of the
requirements for the degrees of

MASTER OF SCIENCE IN MECHANICAL ENGINEERING
and
MECHANICAL ENGINEER

ABSTRACT

An experimental natural convection heat transfer study of a simulated electronic circuit board has been conducted. The board has an array of 9 simulated chips , each dissipating up to 2.5 Watts. The board is immersed in FC75, a fluorocarbon liquid, in an enclosure whose top and bottom surfaces are constant temperature heat sinks. The experimental data have been expressed in terms of relevant dimensionless heat transfer parameters such as Nusselt and Rayleigh numbers. The trend is that, the chips located higher in the enclosure have lower heat transfer rates. Otherwise the chips in the same row behave in a similar way which implies a quasi-two dimensionality.

TABLE OF CONTENTS

LIST OF TABLES

LIST OF FIGURES

NOMENCLATURE

SYMBOL	DESCRIPTION	UNITS
A	Area	m^2
α	Thermal Diffusivity	m^2/ sec
β	Thermal Expansion Coefficient	1/(°C)
c_p	Specific Heat	J/kg-°C
δ	Uncertainty in the Variables	Various
g	Acceleration of gravity	m/ sec^2
Gr	Grashof Number	Dimensionless
h	Heat Transfer Coefficient	W/ m^2-°C
k	Thermal Conductivity	W/ m-°C
L	Characteristic Length	m
Nu	Nusselt Number	Dimensionless
Nu_c	Nusselt Number at Center	Dimensionless
ν	Kinematic Viscosity	m^2/ sec
Pr	Prandtl Number	Dimensionless
Q_{con}	Energy Loss by Conduction	W
Q_{conv}	Energy Added to the Fluid	W
Q_{in}	Energy Input to the Heater	W
R	Resistance of Precision Resistor	Ω's
R_{con}	Total Thermal Resistance	°C/ W
Ra	Rayleigh Number	Dimensionless
Ra_{mc}	Modified Rayleigh Number at Center	Dimensionless
ρ	Density	kg/ m^3
T_a	Ambient Temperature	°C
T_f	Average Film Temperature	°C
T_s	Back Surface Temperature of Component	°C
V_{in}	Input Voltage	Volts
V_h	Voltage Across Heater	Volts

I. INTRODUCTION

A. DESCRIPTION OF THE PROBLEM

Development of electronic packaging, starting with ENIAC, the first digital electronic computer, has created a very urgent need to devise more sophisticated cooling systems. In the last ten years, the remarkable advancement of very densely packaged electronic components has brought about the necessity for enhancement of heat transfer features applied to these thermal packages.

The first electronic packages in 1960's, SSI (Small Scale Integration) chips had only a maximum of 20 devices per chip, whereas today's most advanced ULSI (Ultra High Scale Integration) chips have more than 100,000 devices per chip [Ref. 1.] The overall effect over the past 30 years resulting from this tremendous increase in the packaging densities has been a trend towards ever increasing heat fluxes. While this has always been the case for very high power modules, the same trend towards very high heat fluxes in the microelectronic chips has also been observed. Heat fluxes reaching 10^5 W m^2 on the chip surface have introduced a major cooling problem [Ref. 2]. Inadequate cooling of these elements, coupled with the enviromental temperature rise, often leads to failure of these components and decrease in reliability and performance.

B. BACKGROUND

Many papers on the electronic cooling area have proposed a very wide variety of solutions to specific problems. Major digital technology firms such as IBM, Honeywell and Mitsubishi have become the pioneers in this research area. For instance, air cooling technology of the modules now often includes impingement air cooling to enhance the heat transfer. Using liquid cooled cold plates to conduct heat away from the sources has also been employed. Combined conduction and air cooling has been observed to provide a much higher enhancement when used with fins on the chip surface [Ref. 3].

Some special chip outer surface features such as TPF (Turbulence Promoting Fin) have provided significantly higher cooling enhancements, when used with special gases such as Helium as the closed cycle coolant [Ref. 4]. By doing so, 300% greater dissipation (cooling) level can be reached than when open cycle air is used as the coolant.

Among the cooling techniques mentioned above, liquid forced convection has a very important place since it is possible to attain heat transfer coefficients over an order of magnitude higher than those attainable with air cooling [Ref. 1]. According to TIME magazine, June 17, 1985 issue, the Cray-2 super computer utilizes forced convection with local boiling at some hot spots. In the same magazine it is stressed that "200 gallons of liquid are used in the machine flooding the circuits with a continuous flow of Fluorinert." However, the use of forced convection leads to more complex design features and brings along the possibility of vibration based failure risks.

Finally, more recent advancements and growing use of largescale and very large scale integration (LSI and VLSI) microelectronic technologies with chip dissipation exceeding 1-2 W and chip surface heat fluxes exceeding 10^5 W/m^2 has focused attention on natural convection liquid immersion cooling because of its advantages over forced convection such as simplicity, higher reliability and lower cost [Ref. 5]. Using R-113 as the coolant, different immersion cooling schemes with submerged condensers have been proposed by Bar-Cohen [Ref. 6]. These techniques are mainly based on pool boiling of R-113 or other fluorocarbon liquids in which the components are immersed.

C. STUDIES ON NATURAL CONVECTION COOLING OF ELECTRONIC DEVICES

1. Numerical Studies

Among the different convection heat transfer modes mentioned above, immersion cooling by means of natural convection has received much attention recently because of its high dissipation capabilities, together with such added advantages as no noise and high reliability [Ref. 7]. Starting in early 1960's, numerous studies of natural convection in rectangular enclosures have been carried out. Many of the initial studies were however motivated by applications such as energy transfer within buildings, solar collection etc.. Only recently has computational attention been focused on simulations of natural convection in electronic component cooling.

Acharya et. al [Ref. 8] have investigated the natural convection phenomenon in an inclined square box shaped enclosure which has energy sources in it. Torok [Ref. 9] used finite elements technique to predict component and board temperatures and heat fluxes. Kuhn et. al [Ref. 10] have studied the three dimensional natural convection heat transfer in a rectangular enclosure with heating elements on the verticall wall inside the enclosure. They found that when two elements are

symmetrically placed on the wall, the distance between them has only a little effect on the mean heat transfer rate distribution, but has a significant effect on the local Nusselt Numbers. Shakerin et. al [Ref. 11] have investigated numerically the effect of the discrete roughness elements protruding from the wall of an enclosure. They repeated the numerical procedure for both a single protruding element and two elements.

Liu et. al [Ref. 7] have carried out the finite difference numerical study of natural convection in a rectangular enclosure with an array of chips mounted on a vertical wall. The side walls of the enclosure are assumed to be adiabatic. The result of this numerical study have been presented as temperatures and velocity fields for the enclosure widths of 18 and 30 mm. It was concluded that:

- Temperature field in the enclosure is characterized by boundary layer regions surrounding individual chips.
- There is only small interference among the chips, especially for the lower rows.
- The maximum temperatures on the chip surfaces are located on the upper horizontal faces of the chips. Lesser temperatures have been found on the lower horizontal faces of the chips in the bottom row.
- The results for 30 mm width are essentially the same as those for 18 mm., indicating only a minor dependence on enclosure width.

Liu et. al have also studied the local oscillatory surface temperature responses in the same anclosure [Ref. 12]. This numerical study has shown that the maximum temperatures of chip surfaces have a tendency to fluctuate within a range up to almost $\pm 3\ ^{\circ}C$ with a period of 4 seconds.

2. **Experimental Studies**

Numerous experimental works relating to the enclosure flows have been conducted along with the numerical studies mentioned above. Park et. al [Ref. 13] used thin foil heaters to simulate both flush mounted and protruding microelectronic components. They obtained heat transfer coefficients for various heater heights and widths. Knock [Ref. 2] studied the effect of the location of a single protruding heater in an enclosure, using water as the working fluid. Experiments were conducted with the heater near the bottom, at the center and near the top of a vertical side wall. Side walls were insulated to insure adiabatic boundary conditions on them. He repeated the experimental procedure for three heater locations. The heater position was varied from close to bottom of a side wall to near the top of the side wall. His results can be quantitatively summarized as a trend suggesting that as the heater is raised within the enclosure, the Nusselt number decreases.

Filis et. al [Ref. 14] have investigated the effect of wall temperature nonuniformity on natural convection in an enclosure. They have presented their results stressing that the nonuniform wall temperature is a more realistic boundary condition. Anderson et. al [Ref. 15] have studied the wall roughness effect on heat transfer enhancement in a water filled cubical enclosure.

D. OBJECTIVES

The experimental work described here was motivated by the numerical study by Liu et al. [Ref. 7] and is the basis of the experimental work of this thesis. The objectives of this study are :

- To design and build an enclosure to cool an array of nine simulated chips immersed in FC-75. These simulated chips are to be instrumented with a number of thermocouples, which are to be monitored using a data acquisition system.
- To analyze the data in terms of relevant dimensionless heat transfer parameters such as Rayleigh vs. Nusselt number.
- To prepare a basis for similar future experiments, including various chip configurations and enclosure widths.

II. EXPERIMENTAL APPARATUS

A. GENERAL CONSIDERATIONS

The apparatus used in the experiment consists of an enclosure filled with dialectric liquid. The top and bottom surfaces of the enclosure are formed by two heat exchangers maintained at prescribed temperatures through the use of a water circulation bath. Simulated electronic components are mounted on one of the vertical sidewalls. All other walls are exposed to ambient air. Top view of the enclosure is seen in Figure 2.1.

A simulated circuit board seen in Figure 2.2 contains a 3 by 3 array of symmetrically placed heating elements. The heating element dimensions correspond approximately to those of a 20-pin Dual-in-line-Package (DIP). The dimensions of the heating element used in the present study were identical to those in [Ref. 7] and [Ref. 12] to allow future comparisons between experiments and computations. The heating element was a rectangular parallelopiped made of aluminum with a foil typed heater attached to the bottom face.

The present study dealt with temperature measurements on the surfaces of various heating elements, for a number of different power levels. The temperatures were measured by fine thermocouples attaced to each aluminum block surfaces. The data was acquired using a micro-computer controlled data-acquisition system. Details of the major elements of the experimental assembly are described next.

B. COMPONENTS

1. Heating Element

The heating element is 6 mm wide, 8 mm long and 24 mm high. (Figure 2.3). In order to be able to measure the temperatures of the surfaces, the lateral surfaces are grooved to a 0.5 mm depth to contain thermocouple beads. The front surface of the chip is reached by a hole drilled through the thickness of the component. The beads and other uninsulated parts of the thermocouples are insulated using a thin layer of electrical insulating varnish to insure a high enough electrical resistance between the beads and aluminum block. An electrical contact described above may cause extra bimetallic junctions, resulting in false temperature read-outs. The rest of the groove left from thermocouple bead was filled with a high thermal conductivity epoxy, OMEGA BOND 101. The surfaces of the blocks were smoothed out before the epoxy cured.

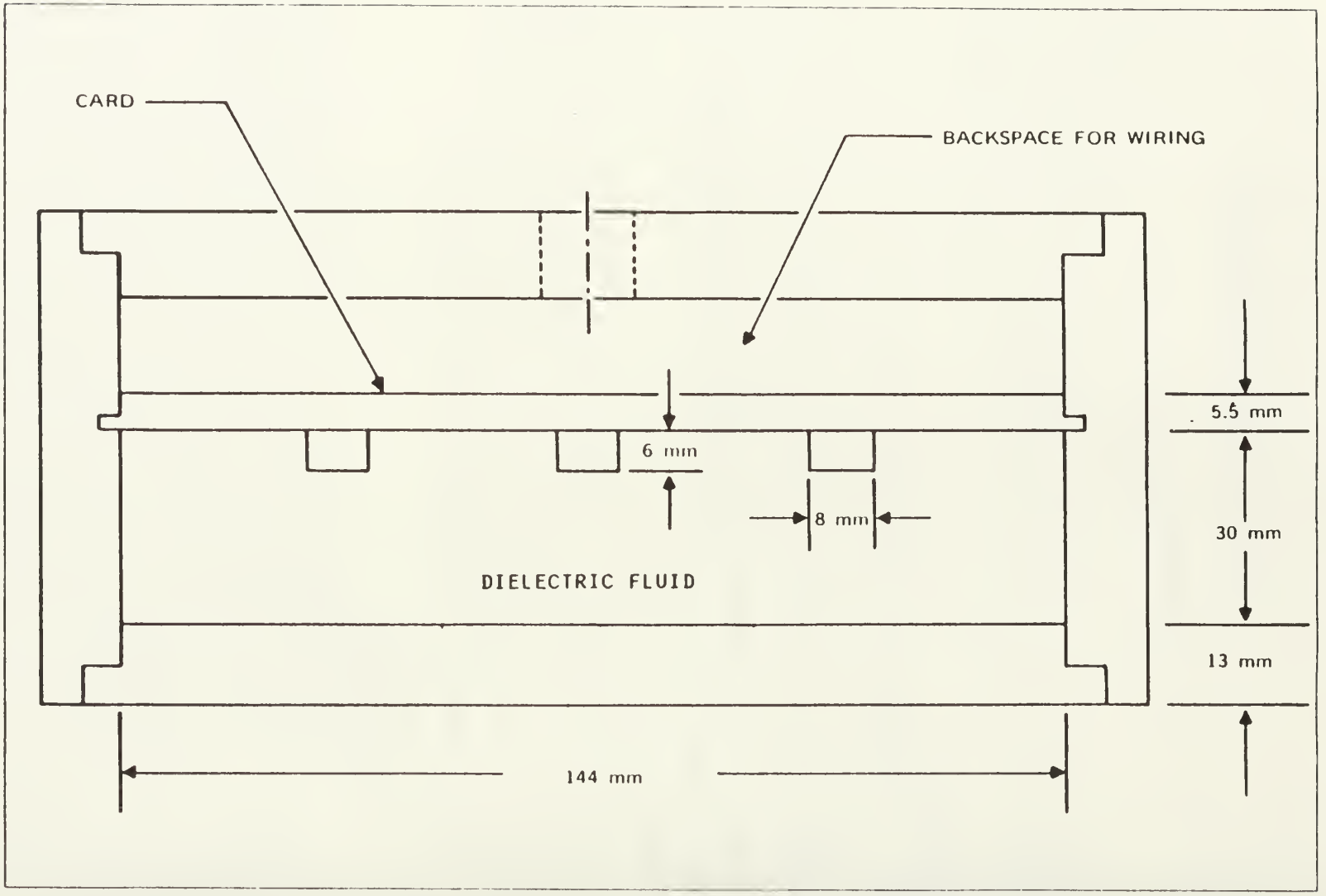

Figure 2.1 Top View of the Enclosure.

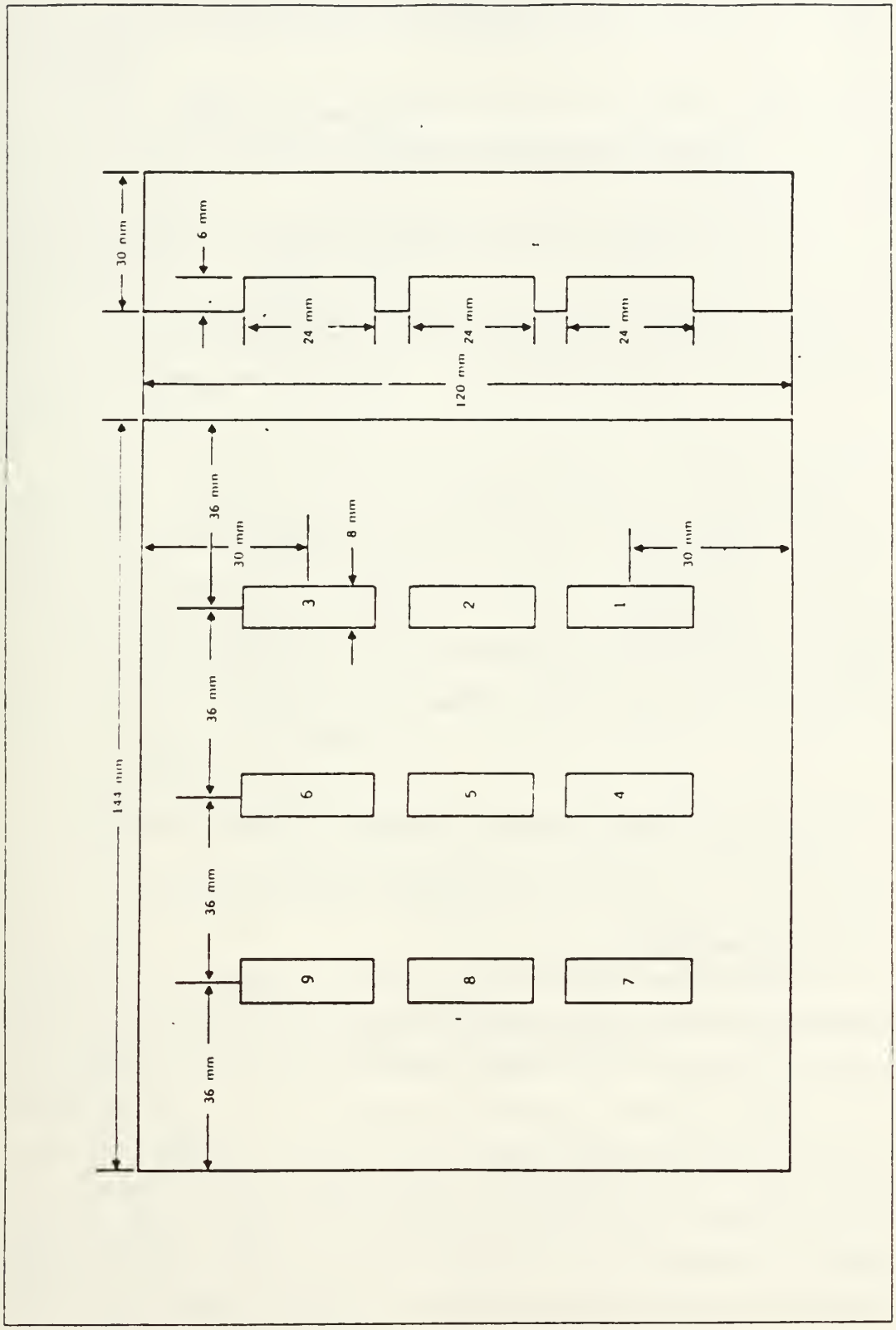

Figure 2.2 Schematic of the Circuit Board.

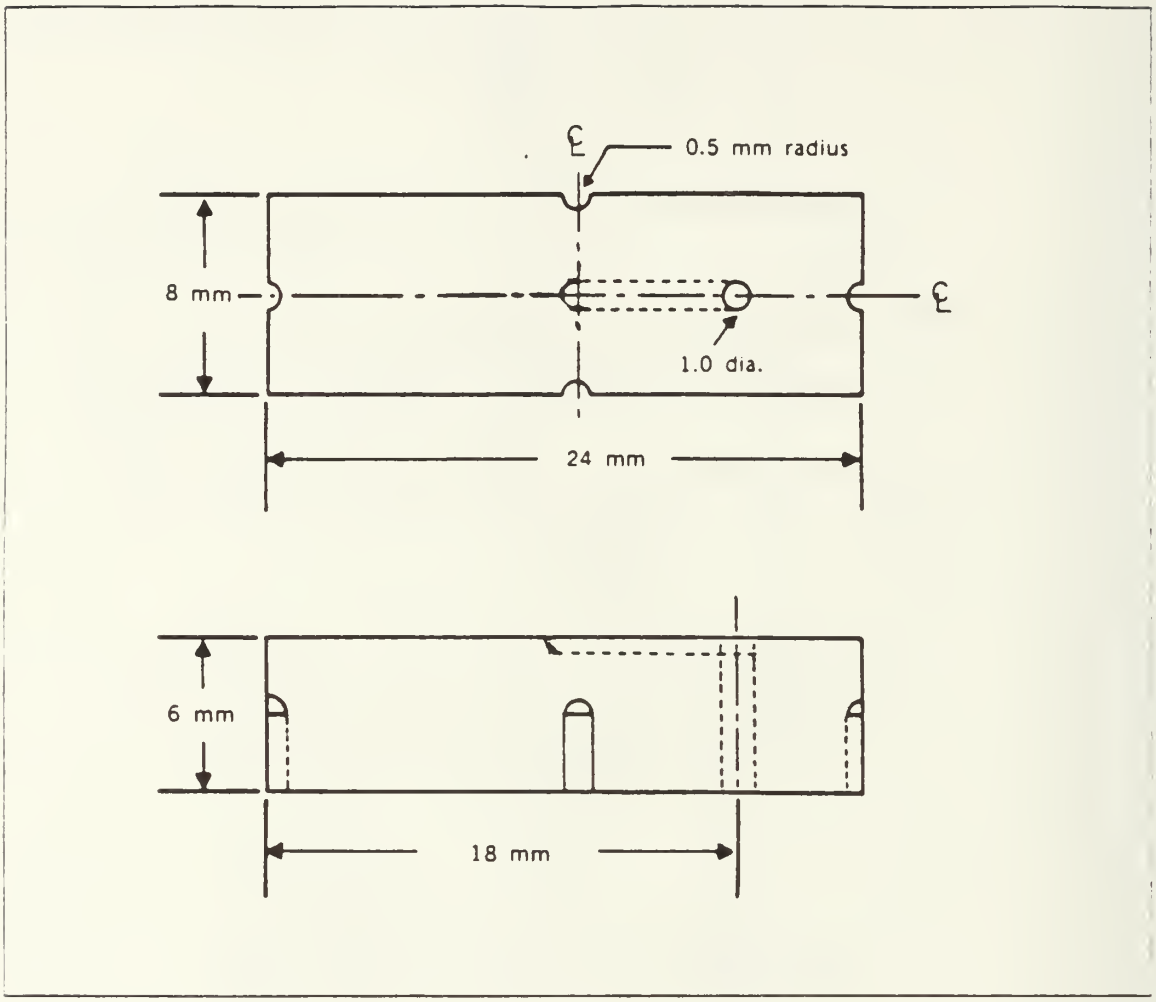

Figure 2.3 Schematic of the Simulated Chip.

2. **Thermocouples**

Because of the relatively small size of the aluminum blocks, a very fine, 3-mil copper-constantan (Omega) thermocouple wire was chosen. By doing so, only a small amount of aluminum had to be drilled out of the entire block (Approximately 7 mm^3 vs. 1152 mm^3, or in other words 0.6% in volume or weight.). Since it is quite difficult to handle these thermocouple wires, special care had to be taken when making the thermocouples. On the thermocouple welder, current and arc time should be set to "minimum" and the argon gas pressure should not exceed 5 psig. The copper wire holder of the welder should be cleaned of carbon build-up with a fine sand paper frequently to maintain the high electrical conductivity to the arc path. Each bead

should be checked for strength before using, since after the cooling off, the bead junction might get brittle and break even if it looks welded.

3. **Heaters**

Marchi Associates foil type heaters were used to provide a nearly constant heat flux boundary condition at the back of the block (Figure 2.4). Each of the resistances were measured to be between 10.5 to 11.8 Ω's. The resistor loop conductor material is Inconel-600. The back of the heater element is laminated with Kapton with a maximum allowable operating temperature of about 250°C. The thickness of the heater element is 0.18 mm. Each of the heater elements has holes at the same locations as the back of the aluminum blocks to pass the thermocouple wire terminating on the front face. In addition, the heating element has four slots on the sides to allow passage of other thermocouples.

The power leads from the heater resistor loops are gold plated to insure low electrical contact resistance on soldering. Wires are soldered to gold plated power lead hook-ups. A length of 5 mm from the bottom of the foil heaters had to be clipped off in order to accomodate a 6 mm distance between blocks. Heaters were bonded to the blocks using OMEGA BOND 100 adhesive epoxy, after making sure that the holes and blocks were lined up by means of a piece of wire. They were then squeezed together in a small hand vice. Teflon sheets were used on both faces of the vice to protect the surfaces of the heater and aluminum block.

4. **Simulated Circuit Board**

The vertical sidewalls containing the heating element are made of a 5.5 mm thick plexiglass sheet. The 120 mm by 144 mm card was grooved at the heater locations to a depth of 0.5 mm to eliminate the extra thickness that would have resulted from the adhesive used to bond both heater to simulated chip and chip to circuit board. The components with heaters were bonded to the card using rubber to metal cement. After placing the thermocouples and clipping off the extra length on the foil heaters, the grooves were filled with OMEGA BOND 101 fast set epoxy and smoothed out.

5. **Test Chamber**

The test chamber is made of 13 mm thick plexiglass which has the dimensions of 120 mm length, 144 mm height and 30 mm width. The spacing at the back is provided to carry the wiring out of the test section. All the wiring was taken out through a Tygon guide tube. Two 3 mm aluminum plates were used as lids for the bottom and the top of the enclosure.

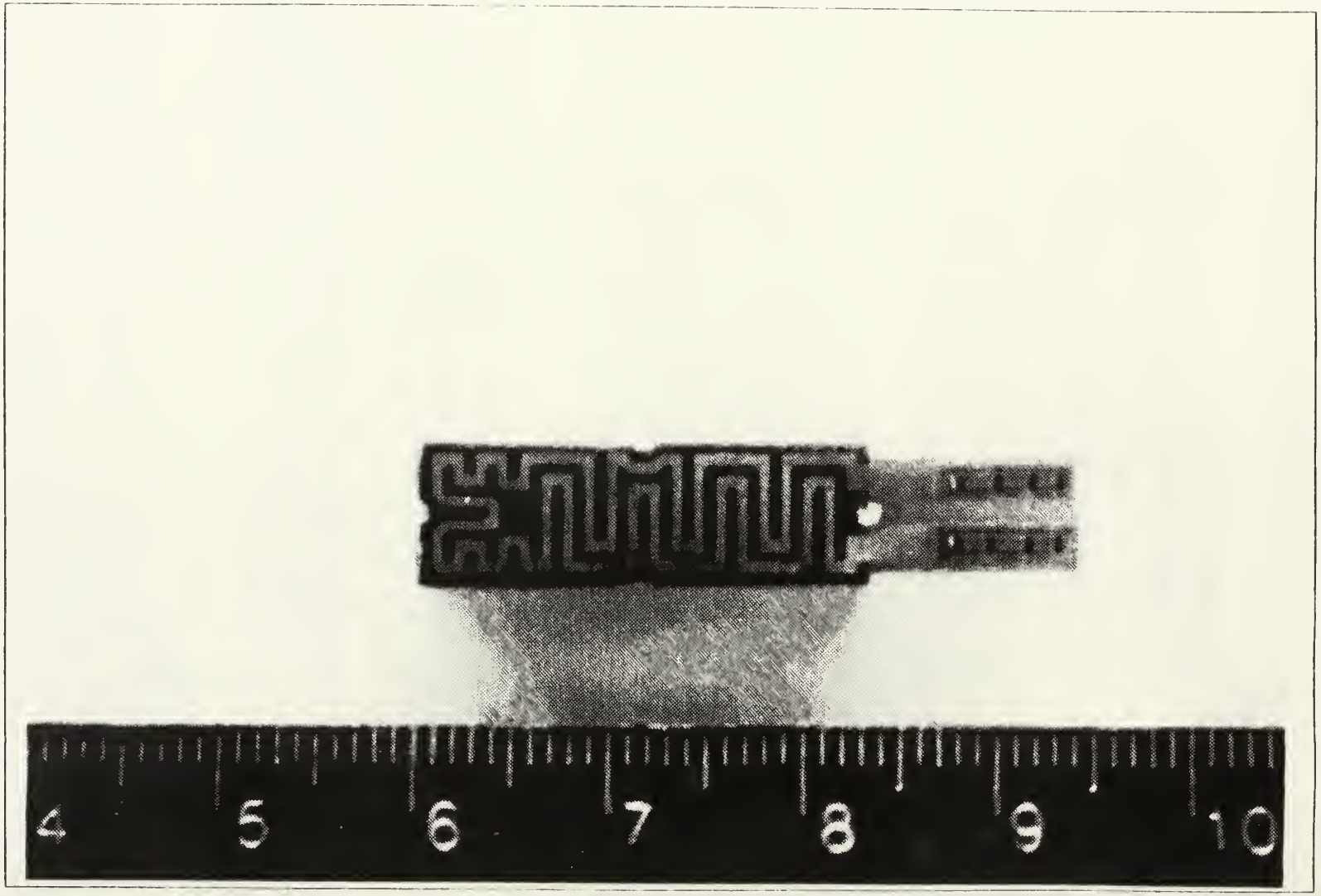

Figure 2.4 Photograph of the Foil Heater with Simulated chip.

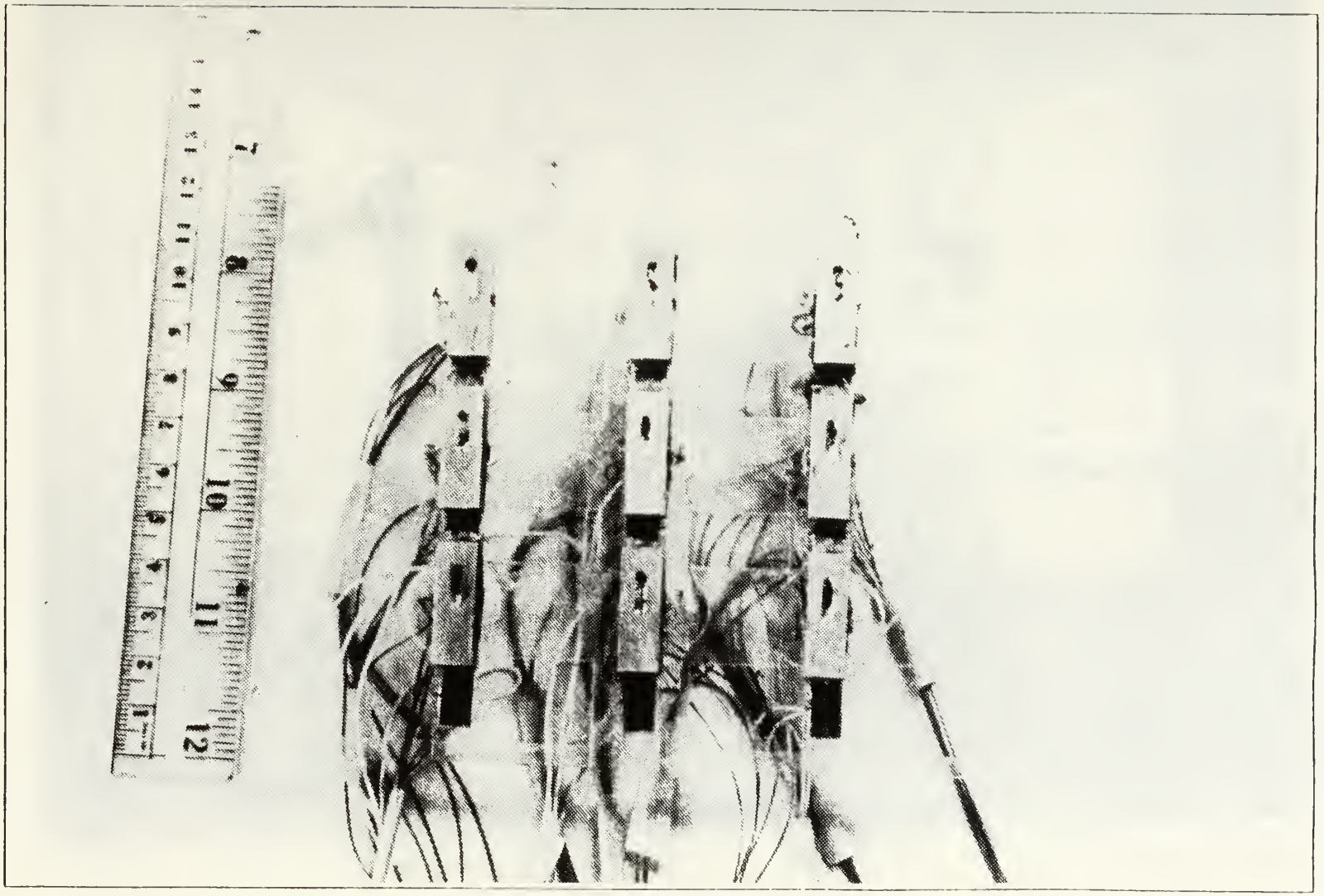

Figure 2.5 Photograph of the Simulated Circuit Board.

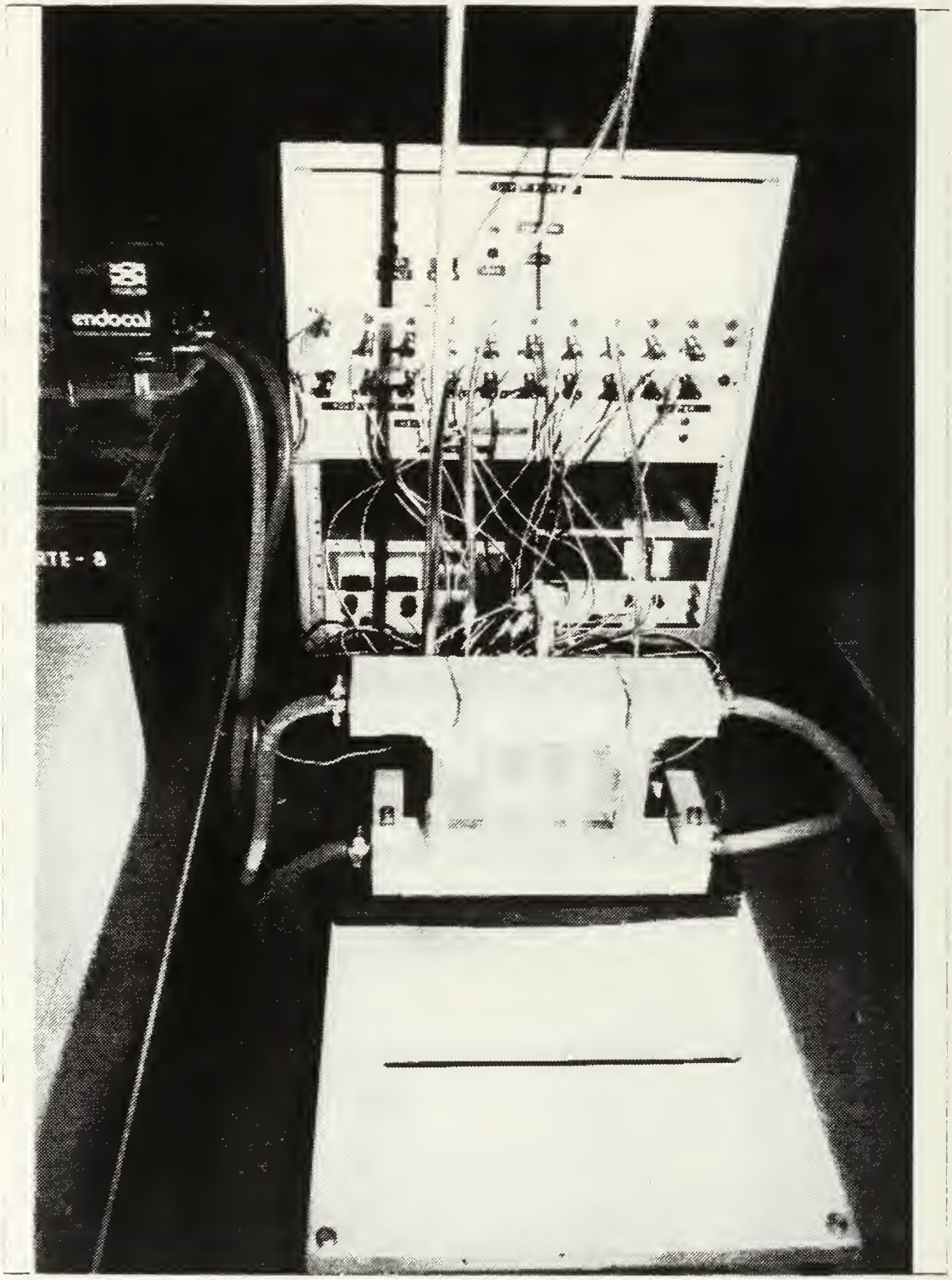

Figure 2.6 Photograph of the Test Chamber.

6. Heat Exchangers

The two aluminum heat exchangers measure 38 mm by 65 mm by 274 mm. The details of the heat exchangers are given in [Ref. 2]. The top and bottom aluminum lids were grooved to a 2.5 mm depth to provide thermocouple slots. This left a 0.5 mm wall thickness of aluminum between the thermocouple bead and the other surface of the aluminum plate. The thermal resistance of the 0.5 mm aluminum wall was neglected. Heat exchangers were fed with water as coolant (in series) by means of tygon tubing. Four 10-mil thermocouples were used to read the top and bottom heat exchanger temperatures.

7. Assembly

After sliding the card into the slot in the enclosure, both thermocouple and power wires were run through a small 1/2 in. diameter extension pipe behind the enclosure and then taken out through a 1/2 in. diameter tygon tube of 25 cm. length. Top and bottom heat exchangers were bonded to the encloure using RTV 732 adhesive/sealant. The back space of the enclosure was filled with rubber pieces to decrease conduction losses to the back of the card. After attaching the heat exchangers to the enclosure, the bottom heat exchanger was fixed on an adjustable level aluminum stand by means of two aluminum clamps. A 4 cm. thick rubber slab was placed between the aluminum stand and the bottom heat exchanger to absorb the vibrations from the ground. Finally, inlet and outlet tygon tubes from the constant temperature bath were connected to the heat exchangers. The level of the apparatus was adjusted by means of the adjustment screws under the aluminum stand.

C. INSTRUMENTATION

1. Power to the Chips

Each of the nine heaters was connected in series with a seperate 2 Ohm precision resistor. The nine elements were connected in parallel to the power supply. Power input to each heating element was calculated from a simultaneous measurement of the voltage drop across the precision resistor and the overall voltage drop. (see Appendix A)

The power panel has one main input and 10 terminals, the last one being a spare terminal in this study. The main input is fed from a DC power supply. (KEPCO 0-100 V, 0-5 A, Mod. JQE 100-5 type)

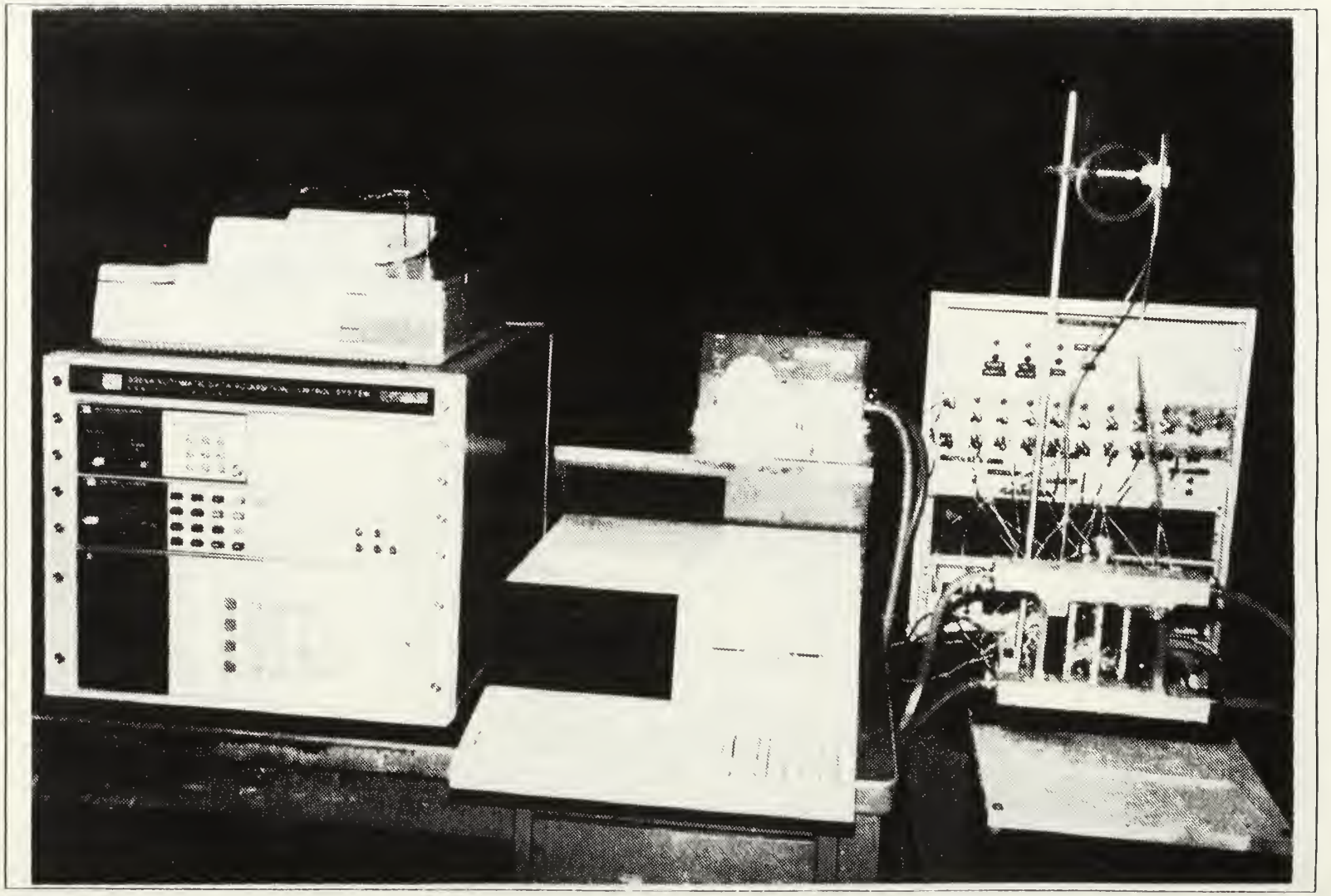

Figure 2.7 Photograph of the Assembly.

2. **Data Acquisition System**

A Hewlett-Packard 3054A Automatic Data Acquisition Control System was used to collect the data. The first 49 channels of the data acquisition system are for the thermocouple readings. Of these, the first forty-five are used for temperature measurements of the heating elements. Channels 46-49 are for the heat exchanger temperature measurements. Channel 50 reads the main input voltage to the power panel. Channels 51-59 read individual heating element voltages.

3. **Computer**

A Hewlett-Packard 9826 computer with Hewlett-Packard 2671A printer was used as the controller for the data acquisition system. Two programs written in HP-BASIC language have the data acquisition system collect the data and store in a data file for each run.

III. EXPERIMENTAL PROCEDURE

A. APPARATUS PREPERATION

After assembling the apparatus, the enclosure was filled through the wire lead tube folded 90° upward, using a small funnel. To damp disturbances from the surroundings, the apparatus is placed on a seperate table. The bubbles inside the enclosure were driven out by laying the enclosure horizontally and tilting it around. After insuring that the liquid is in contact with the top heat exchanger, the enclosure was fixed on the aluminum stand using the aluminum clamps, with a rubber vibration damper in between. The apparatus was then leveled by means of a bubble level placed on the top heat exchanger. Tygon tubing feeding coolant water to the heat exchangers were attached to them in series. In other words, outlet of the top heat exchanger was the inlet of the bottom one. Because of the very high coolant mass flow rate, the temperature drop through the heat exchangers was negligible. Ten terminals on the power panel were used to supply power to the heaters on the simulated chips. The first terminal was the main input, the next nine are the terminals for each heater. They were connected in parallel to the main input with 2Ω resistors which were in series with each heater.

B. DATA ACQUISITION

All the thermocouples were initially scanned to insure that they were reading the same temperature at steady state, for a predetermined sink temperature. The heat exchangers were brought to 21°C by means of the adjustment dial on the constant temperature bath. The voltage on the power supply was next set to the desired level. The voltage setting was calculated knowing that each heater and resistor have a total resistance of approximately 13Ω's. Once the desired power was determined, voltage on the power supply could be set to its approximate value.

Once the voltage on the power supply and the temperature on the constant temperature bath was set to their desired values, all the readings were taken by running the data acquisition program.

Maximum power per component was about 2.35 Watts. At higher values, degasing of the bonding material resulted in bubble formation at the heater blocks. For each seperate power setting, several runs with 1 hour time period were taken.

When the temperature change between two successive readings was within 2%, steady conditions were assumed. This process takes 2-4 hours for each run, depending on the power level.

C. DATA ANALYSIS

For each seperate run, all data were stored in files created by the data acquisition program. After the end of all the runs, steady state data were kept on the disk. These were accessed by a program written for the heat transfer calculations.

All the raw data were used for determining Nusselt and Rayleigh numbers for each chip at each power level.

1. Determination of Nusselt Number

Nusselt Number is defined as following :

$$Nu = \frac{h\ L}{k_f} \qquad \text{(eqn 3.1)}$$

Where L is the characteristic length, taken here as the component height. All the fluid properties were taken variable with average film temperature. In order to evaluate the heat transfer coefficient h, an estimate for conduction loss through the back of the test surface has to be made. A series of conduction thermal resistances, together with a convection boundary condition at the outside wall of the enclosure determines the total heat resistance. (Appendix A)

Conduction resistance R_{con} for each solid layer is determined from :

$$R_{con} = \frac{L}{k\ A} \qquad \text{(eqn 3.2)}$$

Where L is the length along the conduction path, k is the thermal conductivity of the material (see Appendix A) and A is the area normal to the conduction path. Then the conduction loss is :

$$Q_{con} = \frac{T_s - T_a}{R_{con}} \qquad \text{(eqn 3.3)}$$

Power input to each chip is calculated from

$$Q_{in} = \frac{(V_{in} - V_h)V_h}{R} \qquad \text{(eqn 3.4)}$$

Where V_{in} is the input voltage applied to both 2Ω resistor and the heater which is in series with it. V_h is the voltage drop across the heater. The difference between V_{in} and V_h gives the voltage drop on the 2Ω resistor.

The net energy added to the fluid in the enclosure is the difference between Q_{in} and Q_{con} which is at the same time from Newton's law of cooling :

$$Q_{conv} = hA(T_{avg} - T_c)$$
$$= Q_{in} - Q_{con}$$

where,

A = Total surface area of the chip.

T_{avg} = Area weighted average surface temperature.

T_c = average heat exchanger temperature.

Also,

$$T_{avg} = \frac{\sum A_i T_i}{\sum A_i} \qquad \text{(eqn 3.5)}$$

where

T_i = temperature of i^{th} surface of the chip,

A_i = area of the i^{th} surface of the chip. The summation index i, varies from 1 to 5.

The above procedure is repeated for each of the nine chips at each power level. Then, from Equation 3.1, Nusselt number is calculated.

2. **Determination of Rayleigh number**

The definition of Rayleigh number is

$$Ra = (Gr)(Pr)$$

Where

$$Gr = \frac{g\beta L^3(T_{avg} - T_c)}{\nu^2} \qquad \text{(eqn 3.6)}$$

and

$$Pr = \nu / \alpha$$

$$\alpha = k_f/(\rho c_p)$$

All the properties in the above equations are calculated at average film temperature :

$$T_f = \frac{T_{avg} + T_c}{2} \qquad \text{(eqn 3.7)}$$

Functional relationships for the properties at the film temperatures are given in Appendix A, together with the sample calculations. Uncertainty calculations are given in Appendix B.

3. **Flux Based Rayleigh Number**

Another approach is to calculate a modified Rayleigh Number based on the heat flux. This Rayleigh number is defined as:

$$Ra_{mc} = (Gr_{mc})(Pr)$$

Where "c" stands for the center of the heated block.

$$Gr_{mc} = \frac{g\beta L^4 q''}{16 k_f \nu^2} \qquad \text{(eqn 3.8)}$$

where $q'' = Q_{net} A$ is the heat flux at the surface of the chip and ;

$$Nu_c = \frac{h\,L}{2k_f} \qquad \text{(eqn 3.9)}$$

Here

$$h = q'' / (T_{avg} - T_f)$$

The above definition of Ra_{mc} and Nu_c have been used to compare the results with those of Fujii and Fujii [Ref. 23]. Fujii and Fujii correlation of boundary layer solution for a vertical surface with constant heat flux is given by :

$$Nu_c = f(Pr)(Gr_{mc}Pr)^{0.2} \qquad \text{(eqn 3.10)}$$

where

$$f(Pr) = (Pr/(4+9\sqrt{Pr}+10Pr))^{0.2}$$

IV. RESULTS

A. TEMPERATURE DATA

As indicated in Chapter III, the raw temperature data were kept in order to be processed later on by the heat transfer calculations program. Temperature outputs belonging to 6 power levels are as following (see figure 2.2 for identification of chip numbers).

TABLE I

TEMPERATURE DATA FOR INPUT POWER Q_{IN} = 0.34 W

DATA IS STORED IN DATA FILE : DATA7

	CENTER	TOP	RIGHT	LEFT	BOTTOM	POWER(WATTS)
CHIP NO1:	29.4	29.7	29.7	28.9	29.8	.35
CHIP NO2:	31.4	31.6	30.9	29.7	31.1	.35
CHIP NO3:	31.9	32.0	31.9	31.9	32.0	.33
CHIP NO4:	30.0	28.6	29.2	29.4	29.4	.35
CHIP NO5:	31.8	31.6	31.1	31.7	31.0	.35
CHIP NO6:	32.3	32.5	31.4	31.6	32.5	.35
CHIP NO7:	30.1	32.0	29.4	29.4	32.0	.35
CHIP NO8:	31.2	31.1	30.5	30.8	31.3	.32
CHIP NO9:	32.5	31.5	31.3	31.3	32.0	.35

HEAT EXCHANGER TEMPERATURES:	RIGHT	LEFT
BOT:	20.7	20.6
TOP:	20.8	20.7

TABLE 2

TEMPERATURE DATA FOR INPUT POWER Q_{IN} = 0.68 W

DATA IS STORED IN DATA FILE : DATA12

	CENTER	TOP	RIGHT	LEFT	BOTTOM	POWER(WATTS)
CHIP NO1:	34.2	34.8	34.8	33.5	35.0	.68
CHIP NO2:	37.9	37.5	37.0	34.9	37.3	.69
CHIP NO3:	38.9	39.3	39.1	39.1	39.2	.66
CHIP NO4:	35.4	33.0	34.0	34.3	34.3	.68
CHIP NO5:	38.4	38.0	37.3	38.2	37.0	.68
CHIP NO6:	39.3	39.8	37.4	38.0	39.8	.69
CHIP NO7:	35.6	35.1	34.2	34.2	35.4	.68
CHIP NO8:	37.5	37.3	36.4	36.8	37.8	.64
CHIP NO9:	39.8	38.0	37.2	37.2	39.2	.68

HEAT EXCHANGER TEMPERATURES:	RIGHT	LEFT
BOT:	20.8	20.5
TOP:	20.9	20.6

TABLE 3

TEMPERATURE DATA FOR INPUT POWER Q_{IN} = 1.07 W

DATA IS STORED IN DATA FILE : DATA16

	CENTER	TOP	RIGHT	LEFT	BOTTOM	POWER(WATTS)
CHIP NO1:	40.9	41.5	41.5	39.7	42.2	1.08
CHIP NO2:	46.5	45.6	45.2	42.3	46.0	1.09
CHIP NO3:	48.1	48.9	48.5	48.5	48.7	1.05
CHIP NO4:	43.0	38.8	40.9	41.3	41.3	1.08
CHIP NO5:	47.5	46.4	45.7	47.1	45.2	1.08
CHIP NO6:	48.6	49.2	45.5	46.2	49.3	1.09
CHIP NO7:	43.2	41.9	40.9	40.9	42.6	1.08
CHIP NO8:	46.2	45.5	44.5	45.1	46.6	1.02
CHIP NO9:	49.4	47.1	45.6	45.6	48.7	1.09

HEAT EXCHANGER TEMPERATURES:	RIGHT	LEFT
BOT:	21.1	20.6
TOP:	21.2	20.7

TABLE 4

TEMPERATURE DATA FOR INPUT POWER Q_{IN} = 1.65 W

DATA IS STORED IN DATA FILE : DATA22

	CENTER	TOP	RIGHT	LEFT	BOTTOM	POWER(WATTS)
CHIP NO1:	50.0	50.4	50.4	48.8	52.1	1.65
CHIP NO2:	57.5	56.5	56.5	53.6	56.8	1.67
CHIP NO3:	60.0	64.2	62.1	62.1	63.1	1.63
CHIP NO4:	53.5	47.0	50.3	51.3	50.8	1.65
CHIP NO5:	58.7	56.0	56.2	58.1	55.2	1.66
CHIP NO6:	60.6	61.4	57.0	57.2	61.5	1.67
CHIP NO7:	53.8	50.9	50.4	50.4	52.6	1.65
CHIP NO8:	57.2	56.3	54.6	55.5	57.8	1.57
CHIP NO9:	61.8	58.1	56.9	56.9	63.1	1.66

HEAT EXCHANGER TEMPERATURES:	RIGHT	LEFT
BOT:	21.1	20.9
TOP:	21.2	21.0

TABLE 5

TEMPERATURE DATA FOR INPUT POWER Q_{IN} = 1.95 W

DATA IS STORED IN DATA FILE : DATA27

	CENTER	TOP	RIGHT	LEFT	BOTTOM	POWER(WATTS)
CHIP NO1:	55.1	55.7	56.2	52.8	57.6	1.95
CHIP NO2:	63.5	62.4	62.3	59.2	62.5	1.97
CHIP NO3:	66.3	77.2	71.8	72.5	74.8	1.94
CHIP NO4:	59.1	51.8	55.5	56.3	56.0	1.95
CHIP NO5:	65.5	62.2	62.8	64.8	61.7	1.96
CHIP NO6:	66.0	67.5	61.9	62.8	67.3	1.97
CHIP NO7:	59.5	56.2	55.7	56.2	58.1	1.95
CHIP NO8:	63.8	62.4	60.2	61.9	64.3	1.88
CHIP NO9:	68.2	64.7	63.1	63.7	75.5	1.97

HEAT EXCHANGER TEMPERATURES:	RIGHT	LEFT
BOT:	22.2	20.8
TOP:	22.4	20.9

TABLE 6

TEMPERATURE DATA FOR INPUT POWER Q_{IN} = 2.35 W

DATA IS STORED IN DATA FILE : DATA32

	CENTER	TOP	RIGHT	LEFT	BOTTOM	POWER(WATTS)
CHIP NO1:	64.9	64.9	65.5	61.8	67.4	2.35
CHIP NO2:	73.2	71.8	71.8	68.2	72.0	2.38
CHIP NO3:	75.6	83.3	79.5	80.2	81.7	2.35
CHIP NO4:	68.6	60.4	64.8	64.9	65.2	2.36
CHIP NO5:	75.0	71.5	72.1	74.9	71.7	2.37
CHIP NO6:	75.6	76.7	70.7	72.4	76.6	2.38
CHIP NO7:	70.3	65.5	65.5	66.1	68.0	2.35
CHIP NO8:	73.9	72.6	70.3	71.8	74.5	2.26
CHIP NO9:	77.9	72.5	72.9	73.6	82.5	2.37

HEAT EXCHANGER TEMPERATURES:	RIGHT	LEFT
BOT:	23.6	21.0
TOP:	24.1	21.2

Following are the graphical representation of the temperature data given above. The plots are prepared to include the center, maximum and minimum temperatures for each chip at 6 power levels.

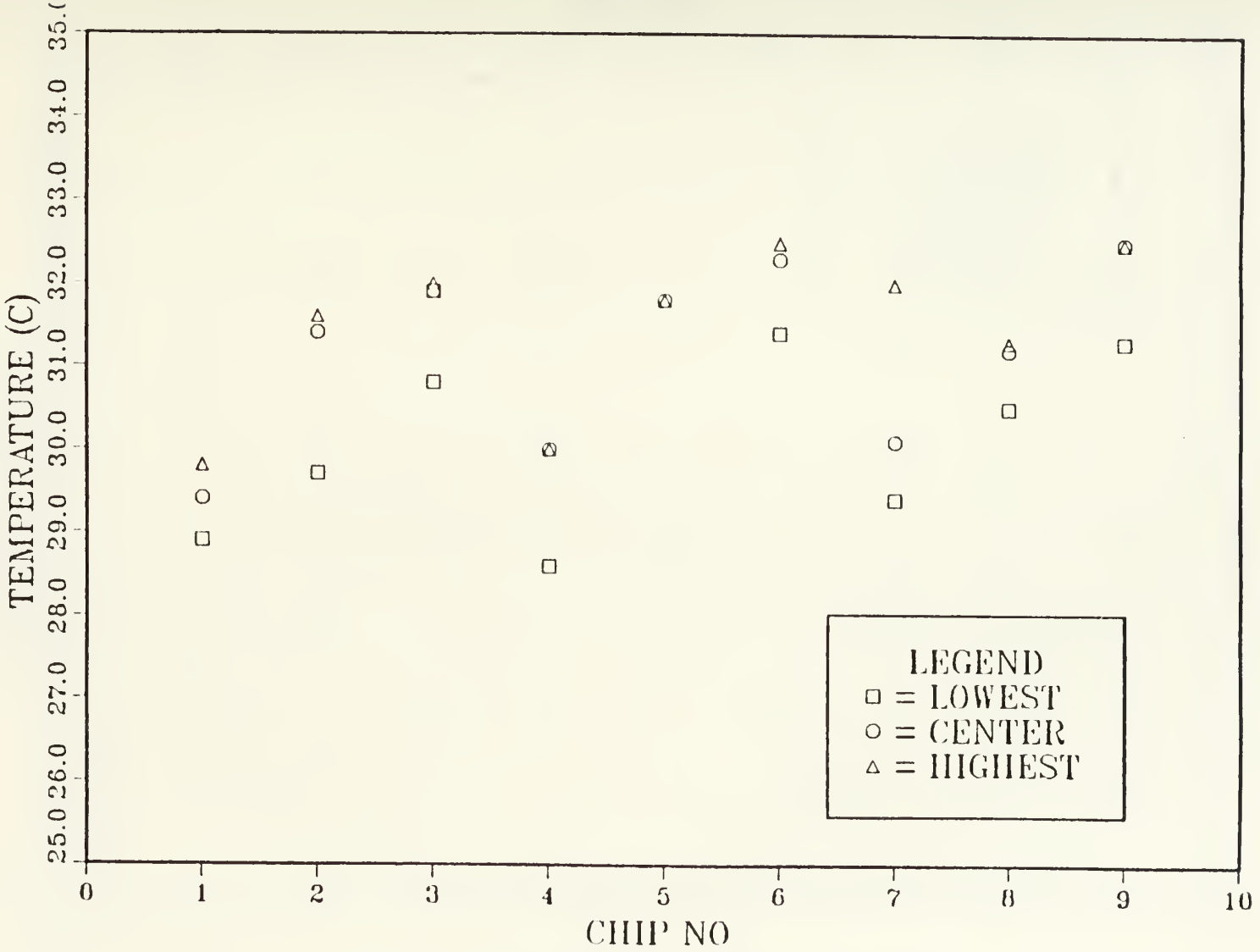

Figure 4.1 Temperature Distribution for Q_{in} = 0.34 W.

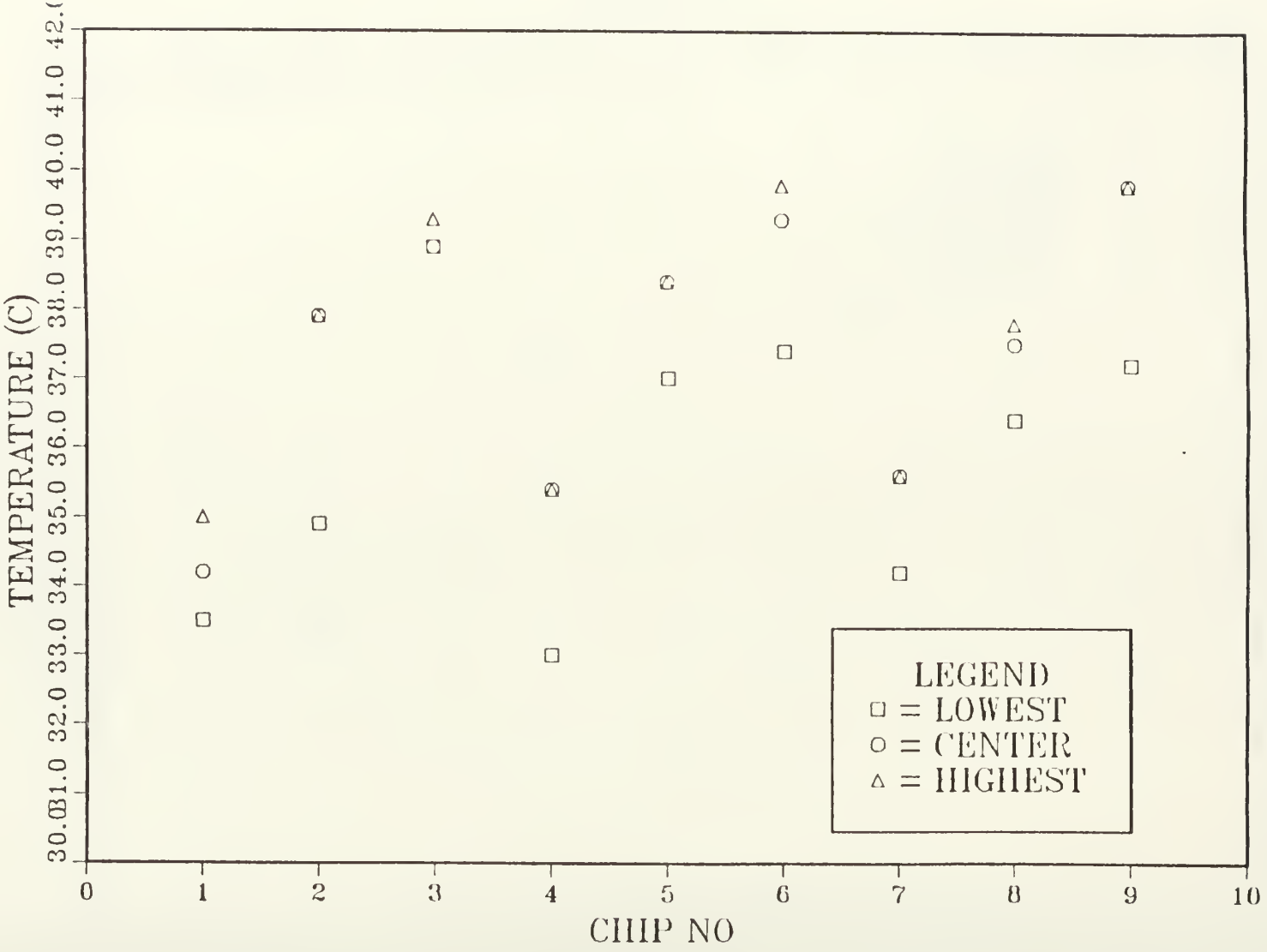

Figure 4.2 Temperature Distribution for Q_{in} = 0.68 W.

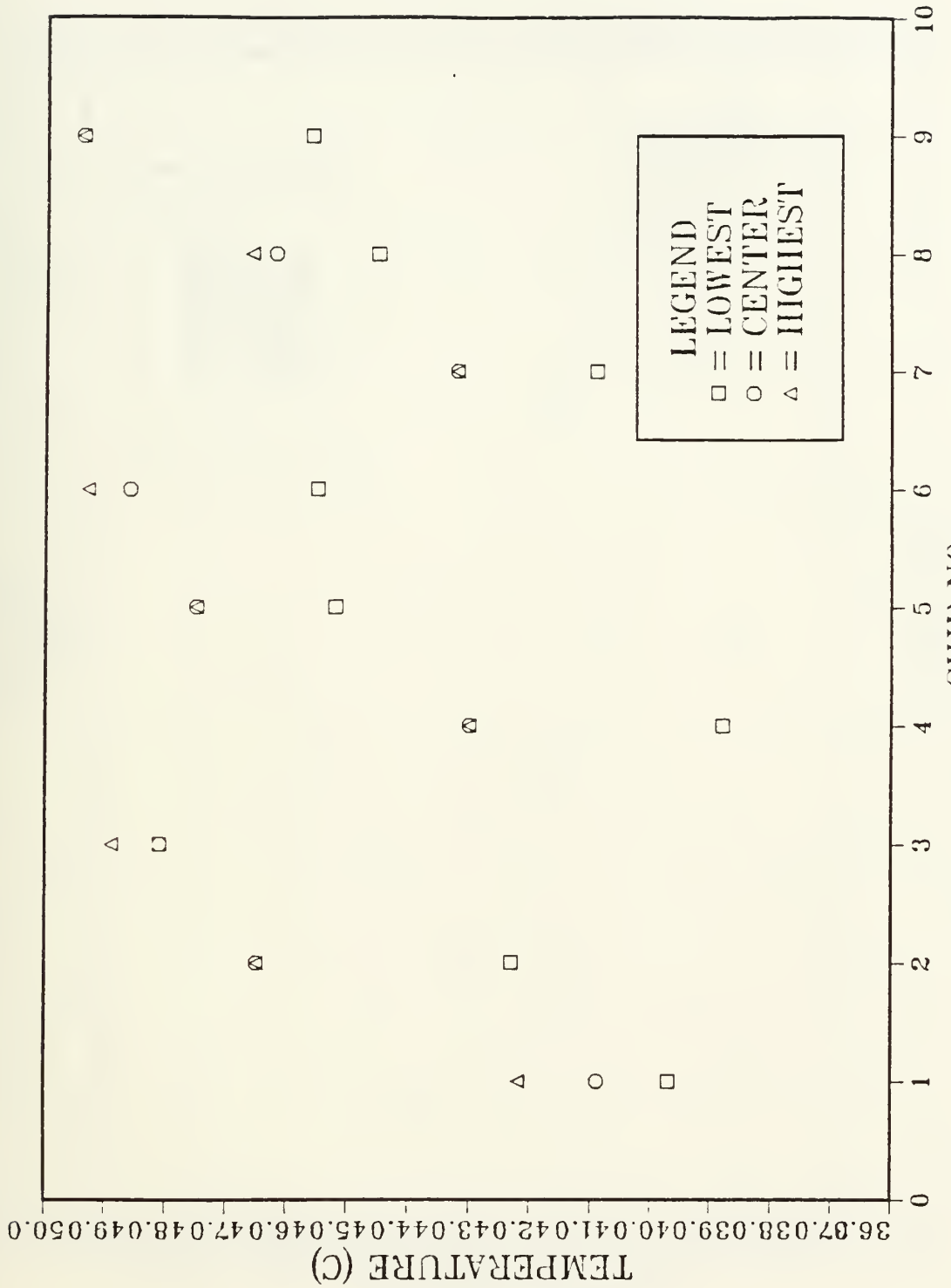

Figure 4.3 Temperature Distribution for Q_{in} = 1.07 W.

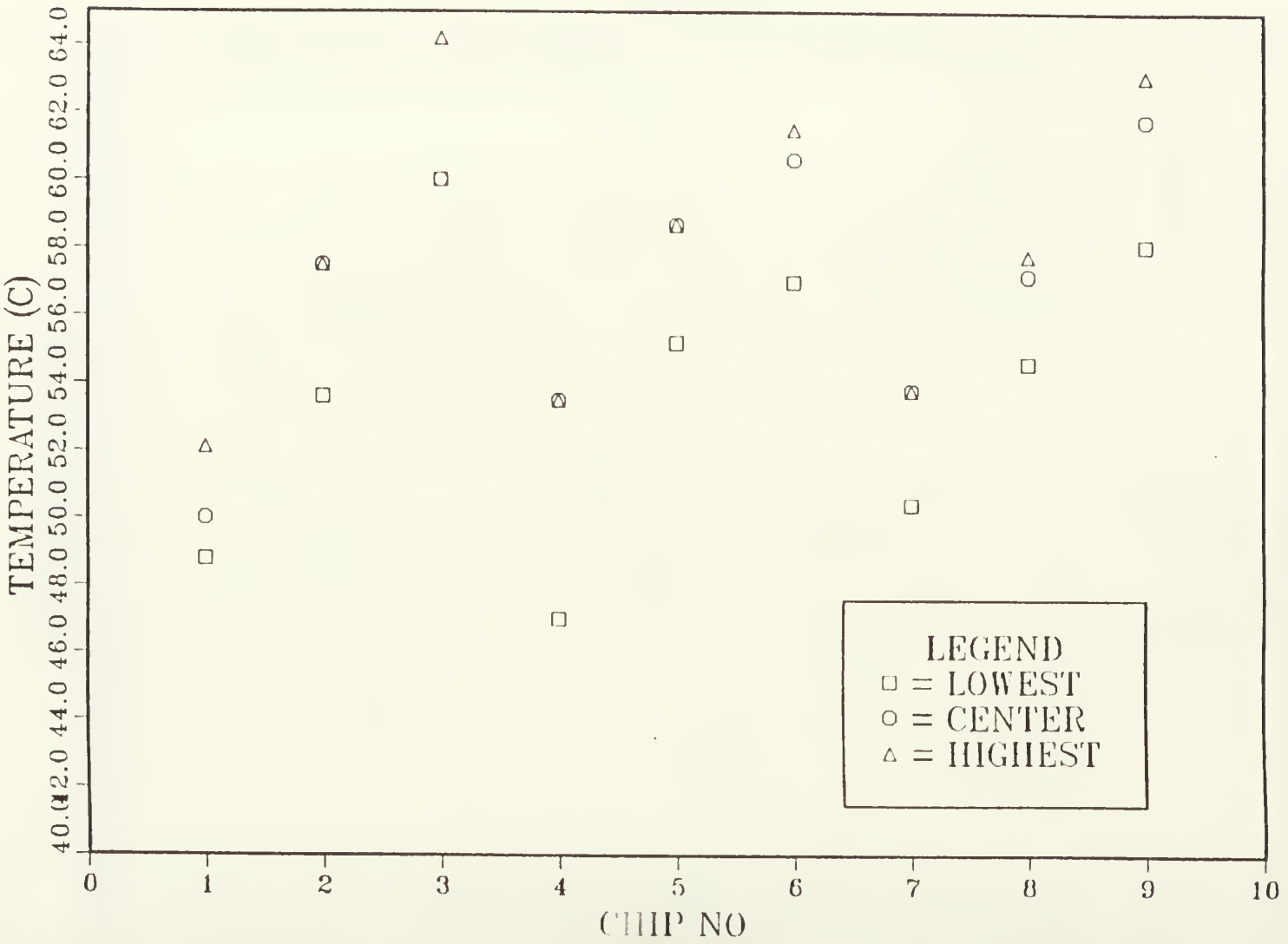

Figure 4.4 Temperature Distribution for Q_{in} = 1.65 W.

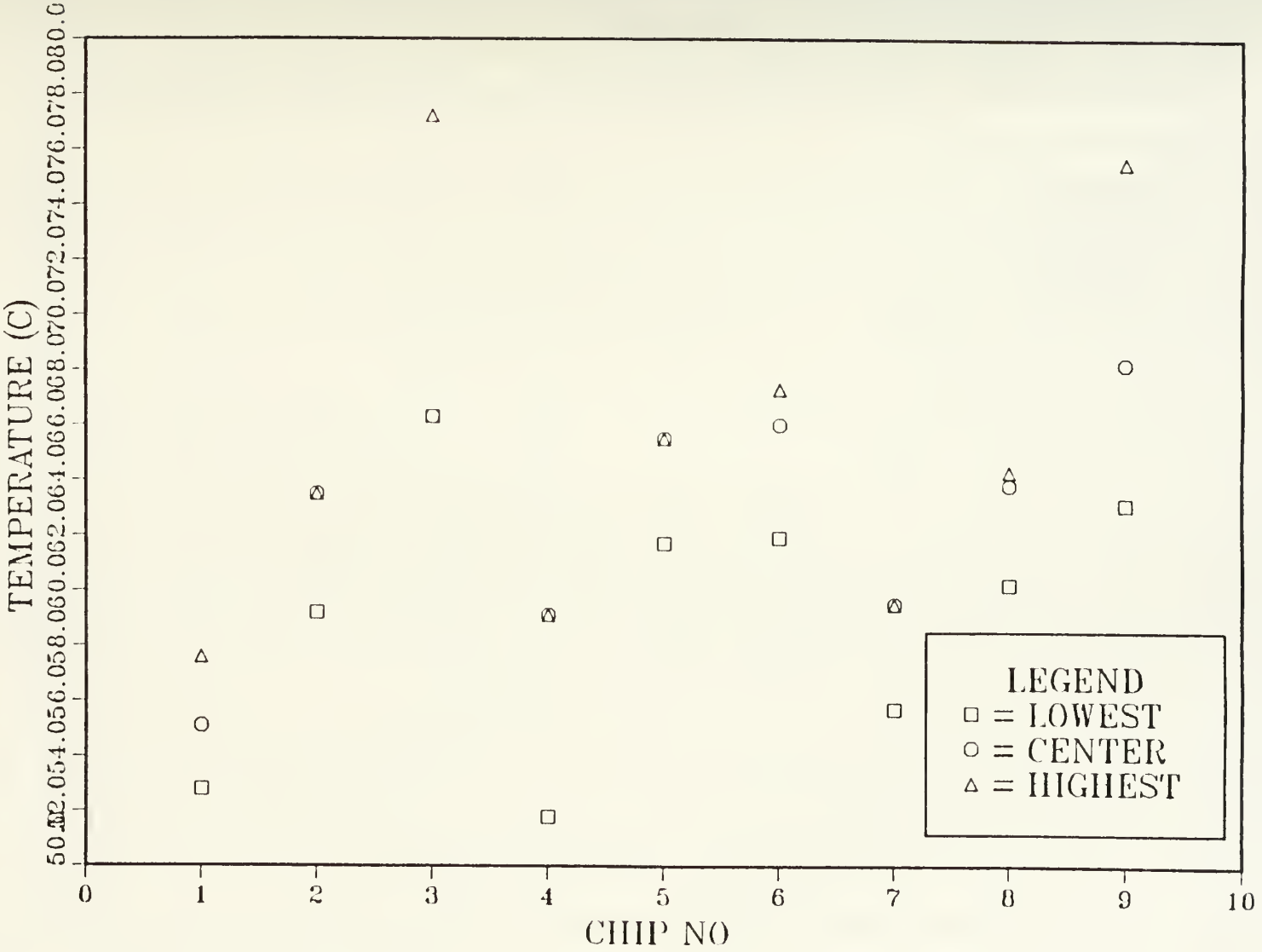

Figure 4.5 Temperature Distribution for Q_m = 1.95 W.

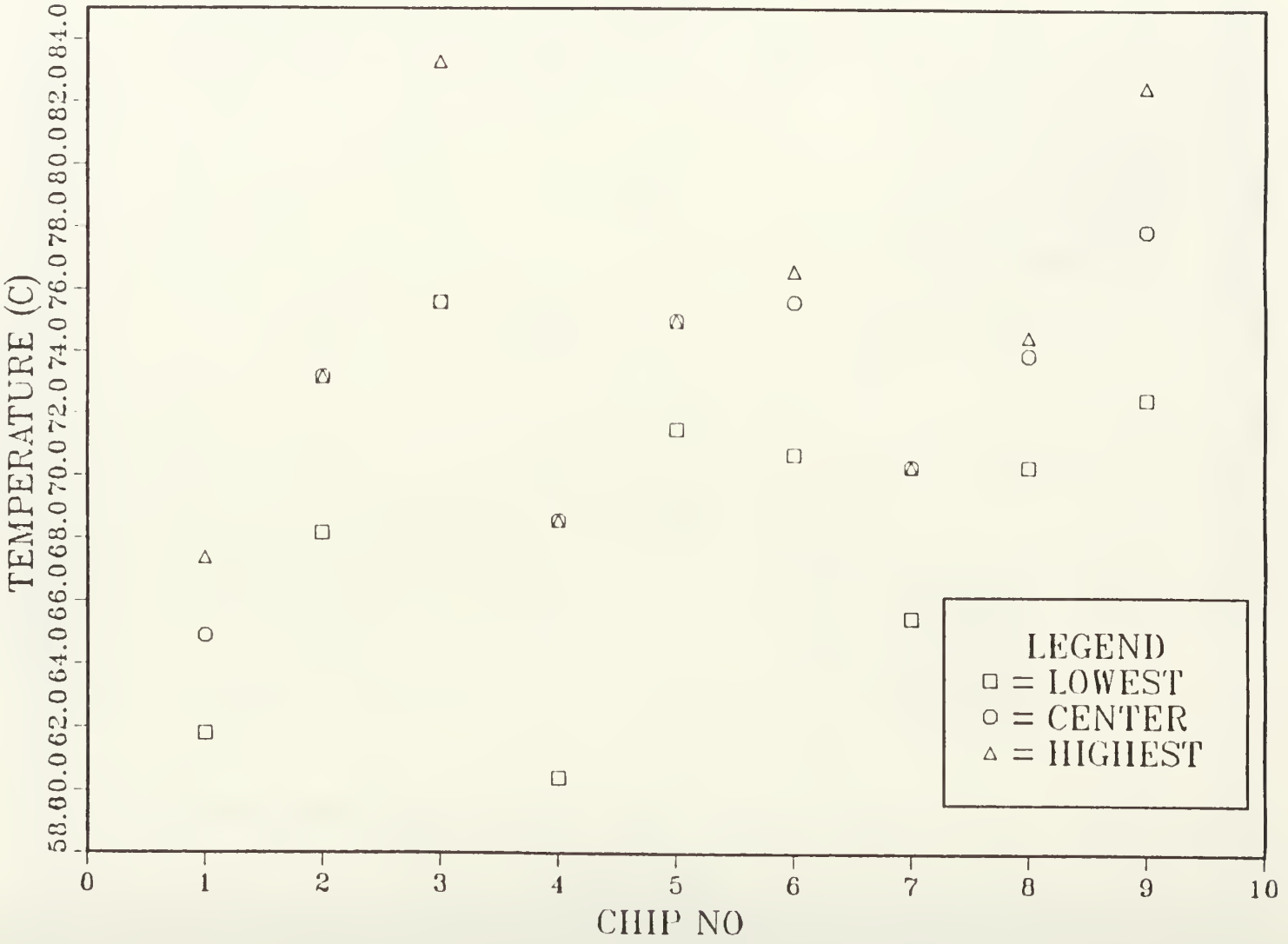

Figure 4.6 Temperature Distribution for Q_m = 2.35 W.

B. HEAT TRANSFER RESULTS

The temperature data given in the previous section have been processed by the heat transfer calculations program given in Appendix C. Following are the tabulation of these heat transfer calculations :

TABLE 7

HEAT TRANSFER CALCULATIONS FOR Q_{IN} = 0.34 W

THE RAW EMF DATA ARE FROM FILE: DATA7

QNET(W)	TAVG-TS	NU	%UNC.IN NU	RA*1.E-7	%UNC.IN RA
.335	8.72	25.38	26.76	5.59	2.89
.299	10.17	19.49	30.73	6.62	2.84
.277	11.26	16.32	33.33	7.41	2.83
.324	8.78	24.37	27.80	5.63	2.89
.292	10.84	17.81	31.76	7.10	2.83
.284	11.25	16.73	32.97	7.40	2.83
.320	9.38	22.55	28.18	6.06	2.86
.283	10.26	18.20	32.18	6.68	2.84
.280	11.08	16.75	33.61	7.28	2.83

TABLE 8

HEAT TRANSFER CALCULATIONS FOR Q_{IN} = 0.65 W

THE RAW EMF DATA ARE FROM FILE: DATA12

QNET(W)	TAVG-TS	NU	%UNC.IN NU	RA*1.E-7	%UNC.IN RA
.662	13.58	32.33	22.10	9.15	2.85
.600	16.16	24.67	25.09	11.16	2.91
.559	18.38	20.22	27.18	12.98	2.99
.639	13.83	30.67	23.01	9.34	2.85
.587	17.26	22.60	25.82	12.06	2.95
.574	17.88	21.35	26.73	12.57	2.97
.636	14.17	29.75	23.16	9.60	2.86
.570	16.38	23.12	26.11	11.34	2.92
.564	17.63	21.26	27.44	12.36	2.96

TABLE 9

HEAT TRANSFER CALCULATIONS FOR Q_{IN} = 1.07 W

THE RAW EMF DATA ARE FROM FILE: DATA16

QNET(W)	TAVG-TS	NU	%UNC.IN NU	RA*1.E-7	%UNC.IN RA
1.054	19.98	35.14	20.93	14.40	3.07
.960	24.11	26.60	23.65	18.07	3.25
.898	27.54	21.83	25.50	21.32	3.41
1.016	20.64	32.79	21.86	14.96	3.10
.936	25.78	24.27	24.45	19.63	3.32
.921	26.42	23.31	25.13	20.24	3.35
1.010	20.99	32.07	22.01	15.27	3.11
.908	24.56	24.70	24.75	18.49	3.27
.906	26.32	23.02	25.74	20.14	3.35

TABLE 10

HEAT TRANSFER CALCULATIONS FOR Q_{IN} = 1.65 W

THE RAW EMF DATA ARE FROM FILE: DATA22

QNET(W)	TAVG-TS	NU	%UNC.IN NU	RA*1.E-7	%UNC.IN RA
1.611	28.99	37.23	20.02	22.80	3.49
1.486	35.11	28.47	22.28	29.20	3.79
1.416	40.61	23.54	23.65	35.48	4.08
1.547	30.37	34.16	21.01	24.18	3.55
1.458	36.39	26.96	22.84	30.62	3.86
1.428	37.97	25.34	23.62	32.41	3.94
1.540	30.72	33.62	21.13	24.54	3.57
1.420	35.07	27.22	23.12	29.16	3.79
1.406	38.11	24.86	24.19	32.57	3.95

TABLE 11

HEAT TRANSFER CALCULATIONS FOR Q_{IN} = 1.95 W

THE RAW EMF DATA ARE FROM FILE: DATA27

QNET(W)	TAVG-TS	NU	%UNC.IN NU	RA*1.E-7	%UNC.IN RA
1.897	33.49	38.08	19.87	27.73	3.77
1.759	40.40	29.39	21.99	35.57	4.13
1.686	49.27	23.23	23.22	46.84	4.62
1.826	35.06	35.05	20.82	29.43	3.85
1.714	42.53	27.26	22.77	38.15	4.24
1.713	42.85	27.04	22.86	38.54	4.26
1.817	35.75	34.22	20.94	30.21	3.88
1.681	40.81	27.82	22.90	36.06	4.15
1.673	44.56	25.42	23.70	40.69	4.36

TABLE 12

HEAT TRANSFER CALCULATIONS FOR Q_{IN} = 2.35 W

THE RAW EMF DATA ARE FROM FILE: DATA32

QNET(W)	TAVG-TS	NU	%UNC.IN NU	RA*1.E-7	%UNC.IN RA
2.257	42.01	36.37	20.41	38.11	4.32
2.125	48.93	29.52	22.17	47.09	4.70
2.062	56.40	24.97	23.04	57.76	5.14
2.192	43.29	34.31	21.16	39.71	4.39
2.082	51.23	27.67	22.77	50.27	4.84
2.080	51.27	27.63	22.86	50.32	4.84
2.159	44.96	32.56	21.58	41.84	4.48
2.020	49.95	27.51	23.24	48.49	4.76
2.037	53.03	26.18	23.59	52.81	4.94

Following are the graphical representation of heat transfer calculations to include Nusselt number versus Rayleigh number. The plots have been classified as BOTTOM row of the chips, MIDDLE row of the chips and TOP row of the chips.

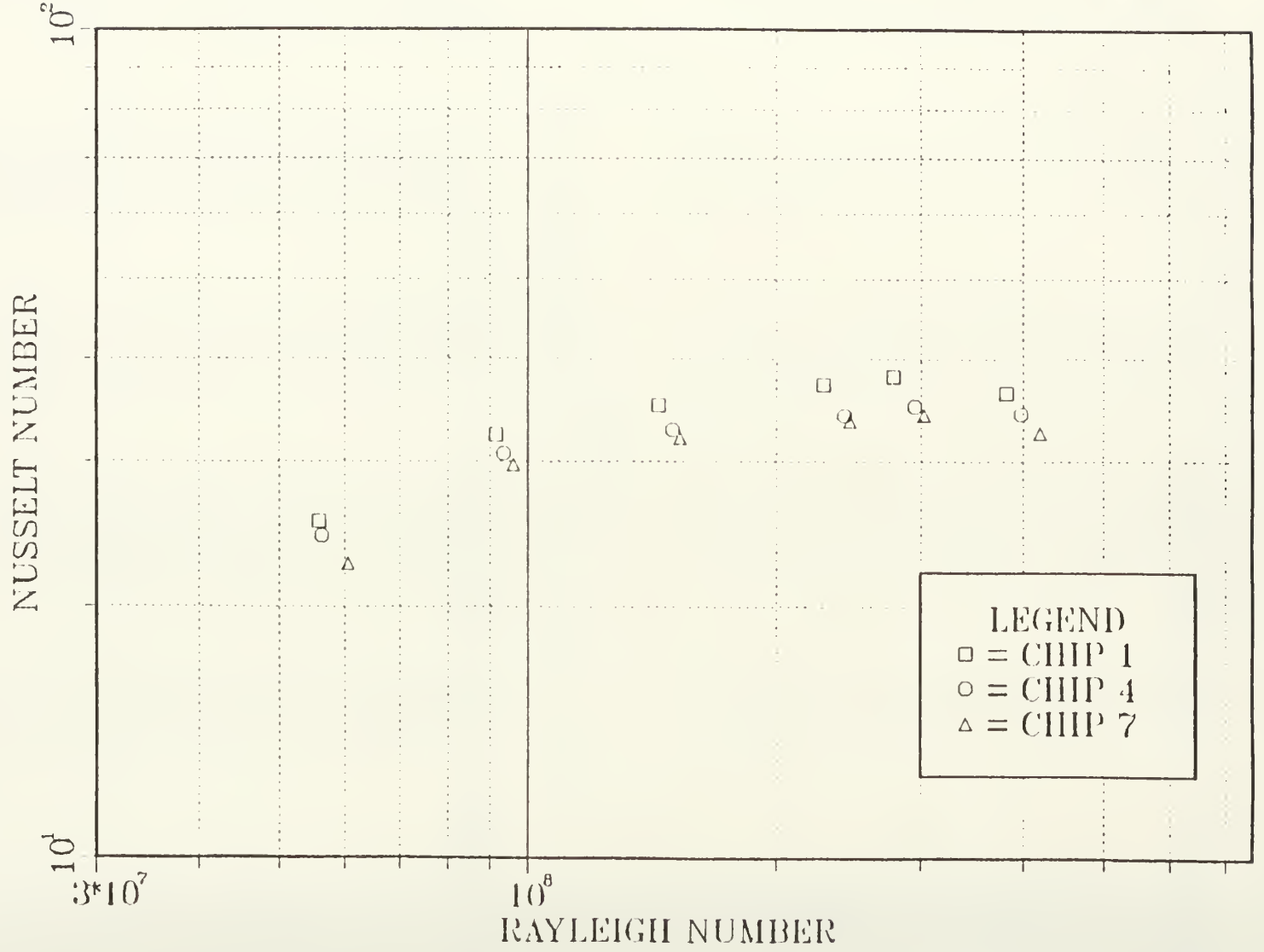

Figure 4.7 Nusselt vs. Rayleigh Number for BOTTOM ROW of the chips.

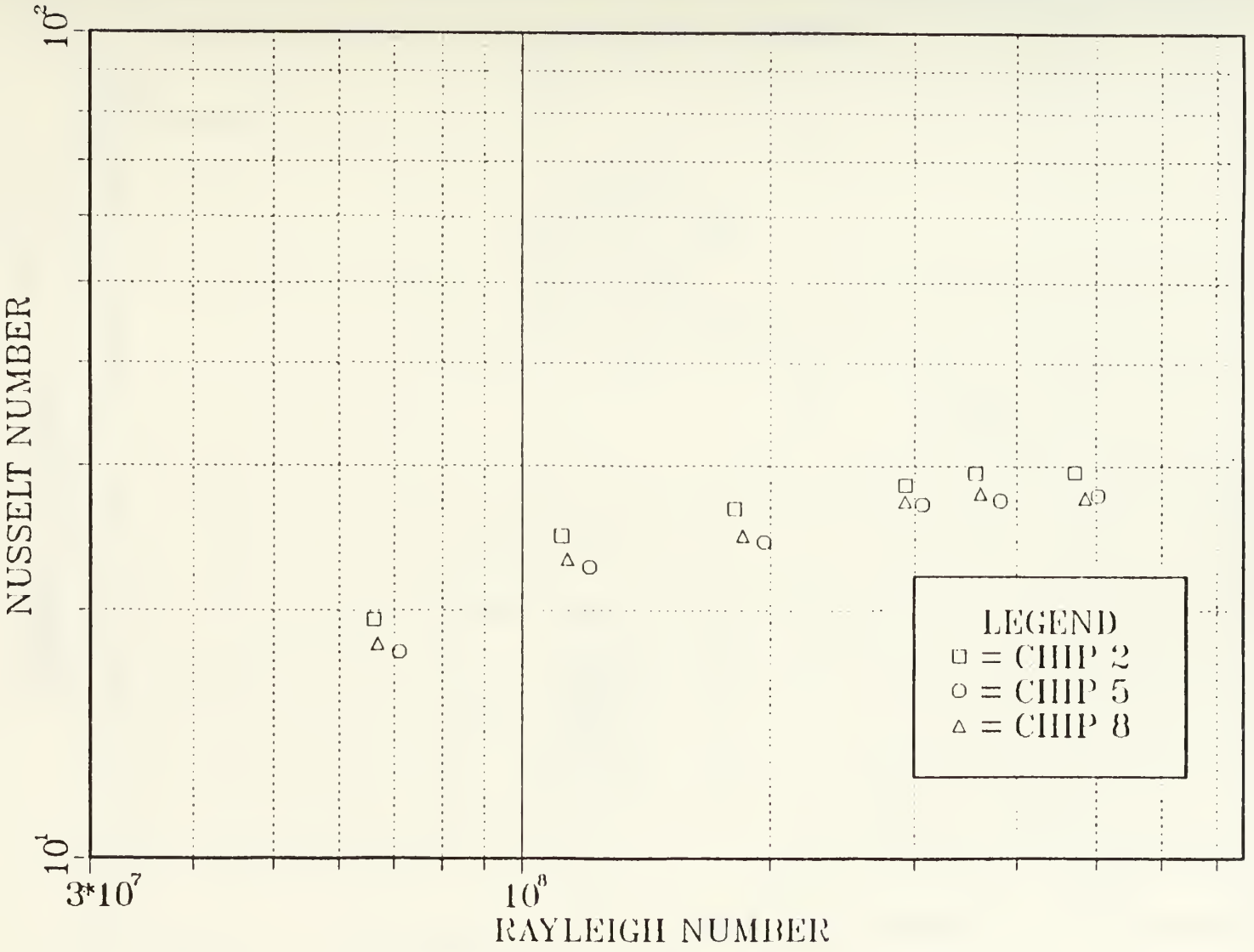

Figure 4.8 Nusselt vs. Rayleigh Number for MIDDLE ROW of the chips.

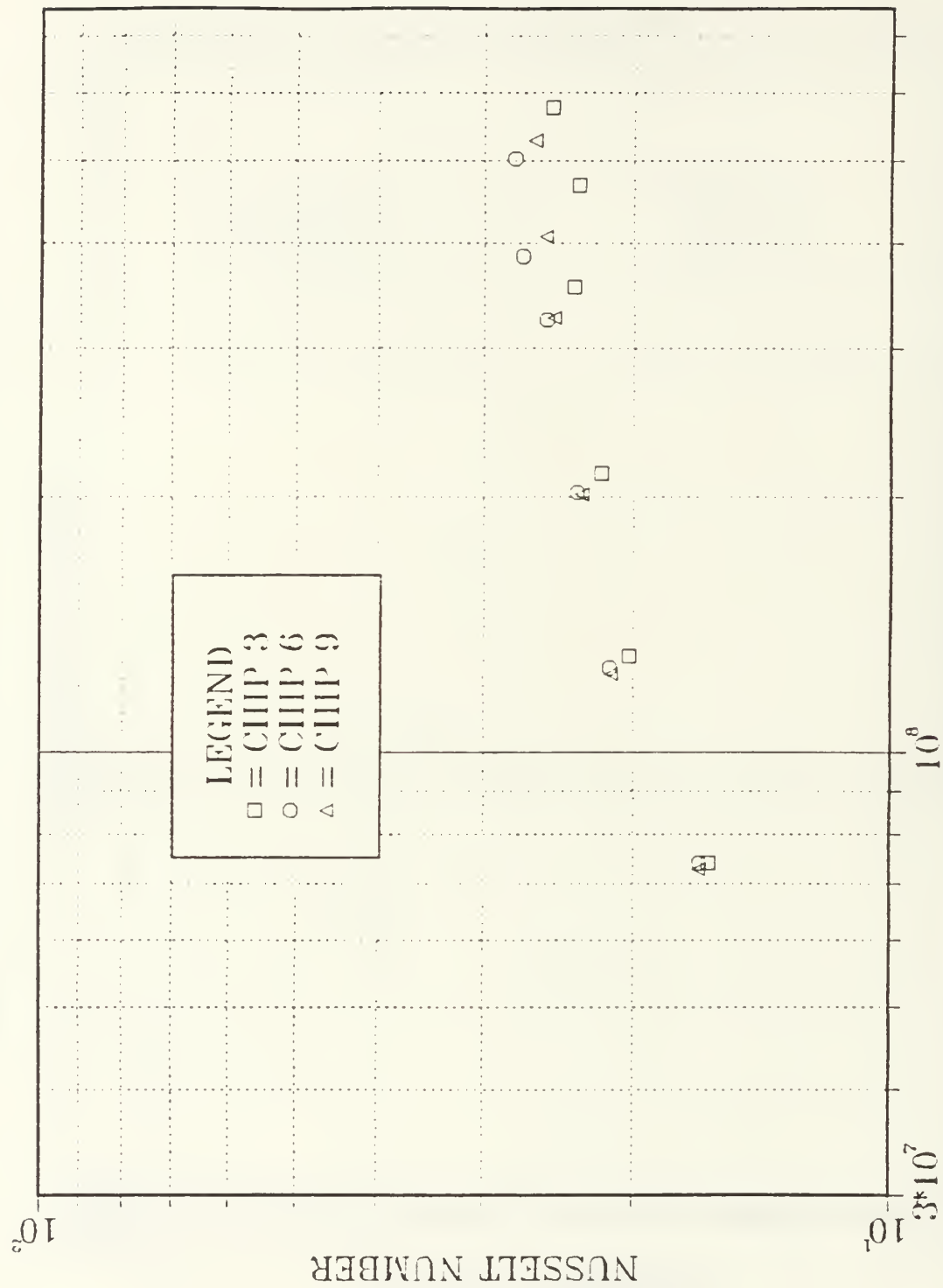

Figure 4.9 Nusselt Number vs. Rayleigh Number for TOP ROW of chips.

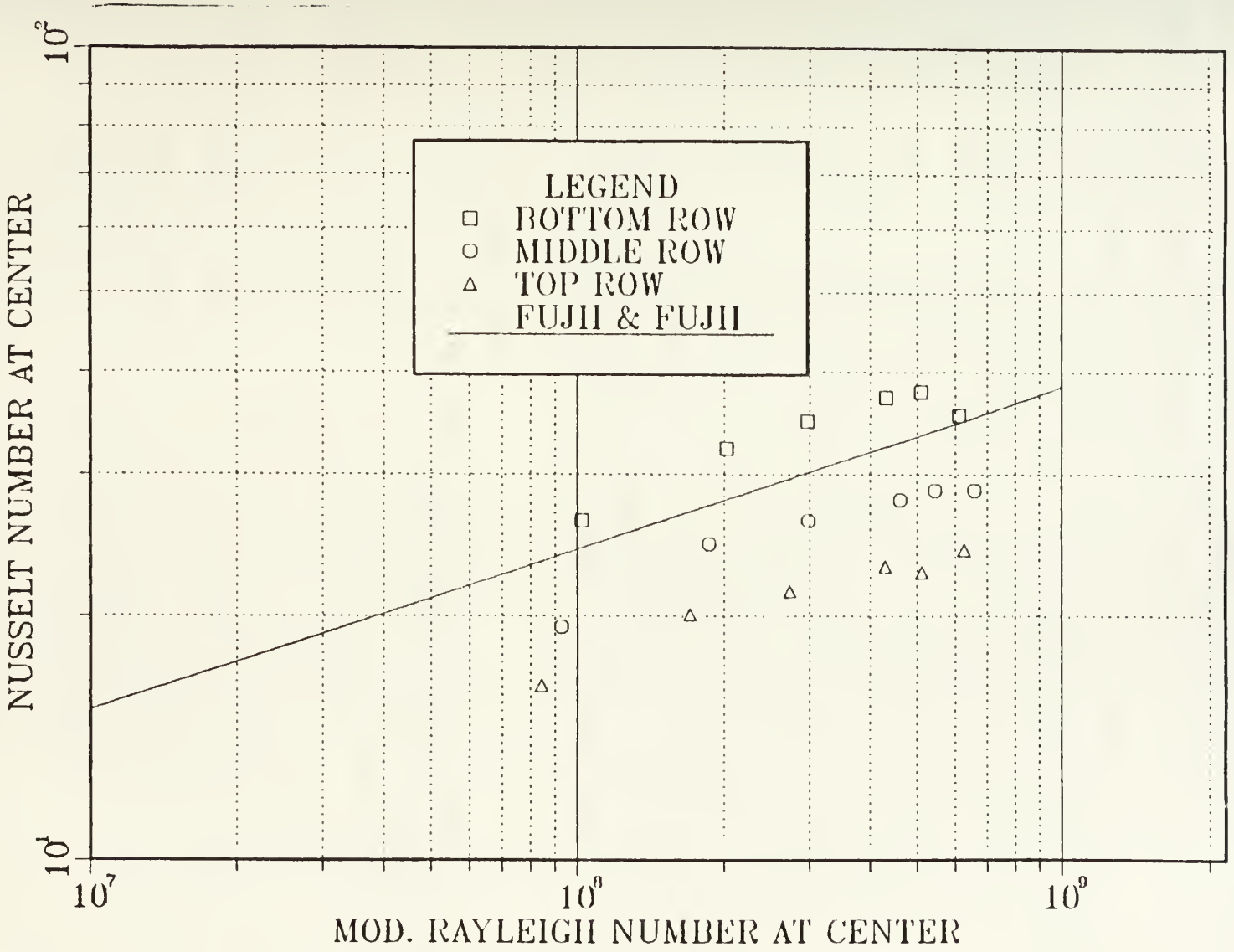

Figure 4.10 Comparison of the Results with Fujii and Fujii Correlation.

Figure 4.10 includes the comparison of the results for chip number 1, 2 and 3 with those of Fujii and Fujii [Ref. 23] in the fashion defined at the end of Chapter III. Fujii and Fujii correlation of boundary layer solutions for a vertical surface with constant heat flux (Equation 3.10) has been applied to mid height of the components.

V. DISCUSSIONS AND RECOMMENDATIONS

A. DISCUSSIONS OF THE RESULTS

Figures including the temperature distribution for different power levels show explicitly that the temperatures of the simulated chips have a tendency to increase with the height inside the enclosure. This suggests that the chips in the bottom row have the lowest temperatures while the top ones have the highest. This conclusion is also obvious from the figures that include Nusselt vs. Rayleigh number. Highest heat transfer rates or in other words highest Nusselt numbers are seen in the lowest row of the chips. Another trend is that the increase in Nusselt number (heat transfer rates) gets smaller with increasing Rayleigh numbers. It is supposed that, this results from the significant increase in the bulk temperature of the fluid. Comparison of the results with Fujii and Fujii correlation [Ref. 23]. shows the weak effect of protrusion on the heat transfer. The bottom row of the chips have a little higher heat transfer rates than those the correlation gives. Especially the top row of the chips have significantly lower heat transfer coefficients. This is because the chips in the bottom row have free boundary layer plumes whereas top row chips have boundary layer plumes confined by those of lower rows.

B. RECOMMENDATIONS

High uncertainty in the Nusselt number calculations results mainly from the necessity to make a rough estimation for conduction losses to the back of the enclosure. This requires that the enclosure walls be very well insulated to insure a very small amount of conduction loss so that the uncertainty is low.

A flow visualization technique for FC-75 should be established. Known techniques for water such as die injection, electro-chemical (because of the requirement for maintaining the dielectricity) or floating particles (because of the requirement for neutral density) techniques are not suitable for FC-75. Repetition of the experiment with different enclosure widths and component configurations will be worthwhile so far as the collection of data sets for general similar problems is concerned.

APPENDIX A
SAMPLE CALCULATIONS

Through this appendix, sample calculations will be based on chip number 2 with power input 0.35 W.

1. DETERMINATION OF INPUT POWER

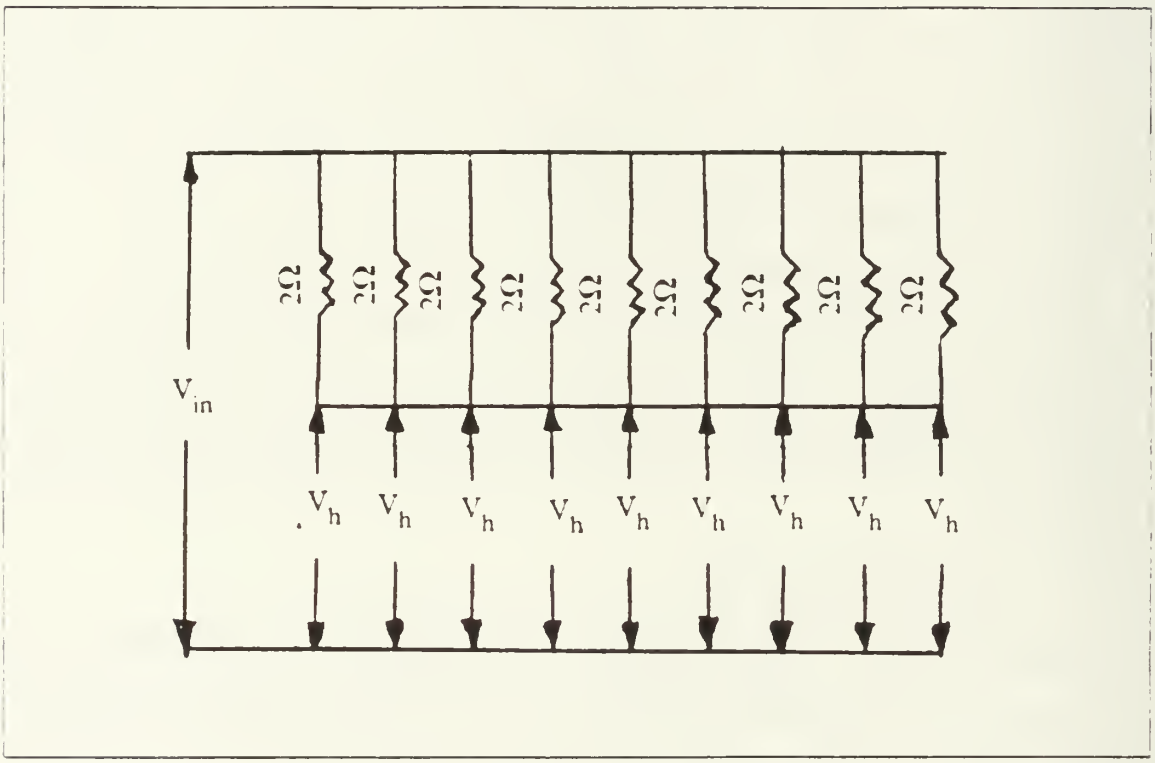

Figure A.1 Electrical Network of Power Input.

From Equation 3.4

$$Q_{in} = (2.377 - 2.032)(2.032)\ 2 = 0.351\ W$$

2. ESTIMATION OF CONDUCTION LOSS

According to Equation 3.3, we need to know T_s and R_{con}. T_s can be calculated using the relationship between Q_{in} and difference between T_s (back surface temperature of the chip) and T_{ce} (center temperature of the chip) obtained from a previous single chip experiment:

$$Q_{in} = 0.083(T_s - T_{ce})$$

Since there are 9 chips, we might want to use an average T_s. From Table 1,

T_s = 35.4°C for chip no 2 and

average T_s = 35.0°C.

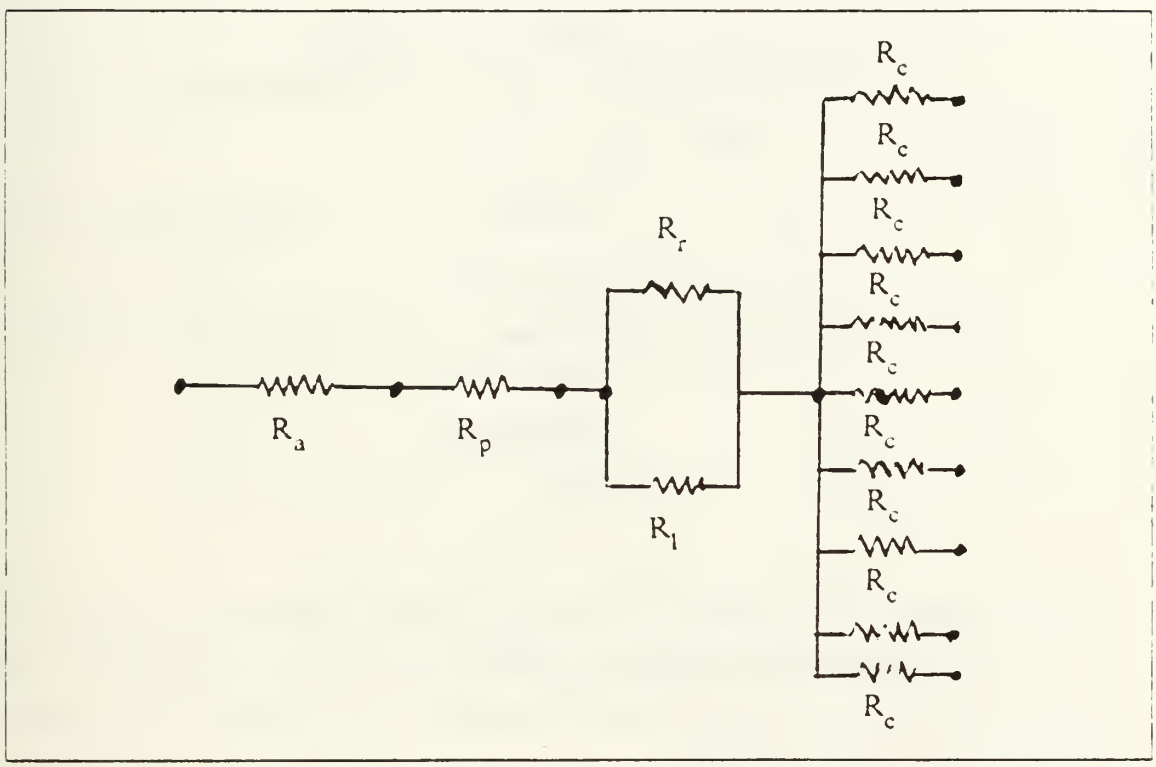

Figure A.2 Thermal Resistance Network for Conduction Loss.

In order to estimate the total thermal resistance R_{con}, we need to know the thermal conductivities of each material, as given in Table 13.

R_a was evaluated from:

$$R_a = (h_a A)^{-1}$$

where h_a = 3.985 W m^{-2}-°C as an average value, calculated from:

$$h_a = 1.42(\Delta T / H)^{0.25} \text{ from [Ref. 22].}$$

TABLE 13
THERMAL CONDUCTIVITIES OF THE MATERIALS

Material	k (W/m-°C)
Rubber	0.0389
Plexiglass	0.1421
FC-75	0.0640

TABLE 14
THERMAL RESISTANCES TO CONDUCTION

Resistance	Material	Value (°C/W)
R_c	Plexiglass	54.979
R_r	Rubber	22.321
R_l	FC-75	54.253
R_p	Plexiglass	4.073
R_a	Air	11.690

R_c was evaluated using a projected area of 16×32 mm^2 instead of 8×24 mm^2. R_r and R_l were evaluated assuming they take up 80% and 20% of the total heat flow area, respectively. Since all the R_c resistances are parallel to each other and, R_r and R_l are parallel to each other such that ;

$$R_{eq1} = 15.814 \text{ °C/W and,}$$
$$R_{eq2} = 6.109 \text{ °C/W}$$

were used. Then the total resistance:

$$R_{con} = 37.686 \text{ °C/W}$$

$\therefore$ from Equation 3.3 :

$$Q_{con} = (35.0 - 20.0)/37.686 = 0.398 \text{ W.}$$

Since, at the same time,

$$Q_{con} = (T_1 - T_a)/R_t$$

where T_1 is the temperature of the back of the circuit board and,

$$R_t = R_{con} - R_{eq2}$$
$$= 31.577\ ^\circ C/W.$$

$\therefore T_1 = 32.57^\circ C$. Then, for chip 2,

$$Q_{con} = (35.4 - 32.57)/54.979 = 0.052\ W.$$

3. CALCULATION OF NUSSELT AND RAYLEIGH NUMBER

From the definitions given in Chapter III,

$$T_c = 20.7^\circ C$$
$$T_{avg} = 30.87^\circ C \text{ and,}$$
$$Q_{conv} = 0.351 - 0.052 = 0.299\ W, \text{ the net power.}$$

Then from Equation 3.3,

$$h = 0.299/(5.76 \times 10^{-4})(30.87 - 20.7)$$
$$= 51.042\ W/m^2\text{-}^\circ C$$

From Equation 3.7,

$$T_f = (30.87 + 20.70)/2 = 25.79^\circ C$$

Using the functional relationships given in [Ref. 7] for properties of FC-75,

$$k_f = 0.1(0.65 - 7.8947 \times 10^{-4}\ T_f)$$
$$= 0.0629\ W/m\text{-}^\circ C$$
$$\rho = 1000(1.825 - 0.00246T_f)$$
$$= 1761.6\ kg/m^3$$
$$c_p = 4180(0.241111 + 3.7037 \times 10^{-4}T_f)$$
$$= 1047.8\ J/kg\text{-}^\circ C$$
$$\nu = 10^{-6}(a_0 + a_1T_f + a_2T_f^2 + a_3T_f^3 + a_4T_f^4)$$
$$= 0.8526 \times 10^{-6}\ m^2/s$$

where

$a_0 = 1.4074$

$a_1 = -2.964 \times 10^{-2}$

$a_2 = 3.8018 \times 10^{-4}$

$a_3 = -2.7308 \times 10^{-6}$

$a_4 = 8.1679 \times 10^{-9}$

$$\beta = 0.00246/(1.825 - 0.00246T_f)$$
$$= 0.0014\ (^\circ C)^{-1}$$

Then, from Equation 3.1 :

$$Nu = (51.042)(0.024)\ 0.0629 = 19.48$$

$$\alpha = (0.0629)/(1761.6)(1047.8) = 3.4077 \times 10^{-8} m^2\ s$$

$$Pr = (0.8526 \times 10^{-6})/(3.4077 \times 10^{-8}) = 25.02$$

From Equation 3.6,

$$Gr = (9.81)(0.0014)(0.024)^3(30.87 - 20.70)/(.8526 \times 10^{-6})^2$$
$$= 2.651 \times 10^6$$

then,

$$Ra = (2.651 \times 10^6)(25.02) = 6.63 \times 10^7$$

Following is to show how Ra_{mc} and Nu_c are calculated;

From Table 7 ,

$$Q_{net} = 0.299\ W.$$

$$q'' = 0.299/5.76 \times 10^{-4} = 519.1\ W/m^2,$$

$\therefore$ from Equation 3.8,

$$Gr_{mc} = 3.70 \times 10^6 \text{ and,}$$

$$Ra_{mc} = 9.26 \times 10^7$$

From Equation 3.9,

$$Nu_c = 19.4$$

in which

$$h = 102.2\ W/m^2\text{-}^oC$$

From Equation 3.10,

$$Nu_c = (0.6088)(39.201) = 23.9$$

APPENDIX B
UNCERTAINTY CALCULATIONS

Uncertainties in the experiment were evaluated using the root mean square method of Kline and McClintock [Ref. 21].

Following is a summary of the uncertainties used in the experiments :

TABLE 15
UNCERTAINTIES OF THE VARIABLES USED IN THE EXPERIMENT

Variable	Uncertainty	Reference
L	10^{-5} m	Resolution of measurement device
T	0.2°C	Thermocouple reading
k_r	5%	[Ref. 2]
k_p	7%	[Ref. 2]
R	0.06Ω	3% variation
k_f	4%	[Ref. 7]

Uncertainty in thermal resistances is given by :

$$\delta R/R = ((\delta L/L)^2 + (\delta k/k)^2 + (\delta A/A)^2)^{0.5}$$

where

$$\delta A/A = ((\delta L_1/L_1)^2 + ((\delta L_2/L_2)^2)^{0.5}$$

For R_p ,

$L_1 = 0.120$ m.

$L_2 = 0.144$ m.

$A = 1.728 \times 10^{-2}$ m^2

$$\therefore \delta A/A = 0.0001, \text{ and ;}$$

$$\delta R/R = 0.07$$

$$\therefore \delta R_p = (4.073)(0.07) = 0.2851 \ ^{\circ}C/W.$$

If similar method is repeated for all the thermal resistances ;

$$\delta R_{con} = ((\delta R_{eq1})^2 + (\delta R_{eq2})^2 + (\delta R_p)^2 + (\delta R_a)^2)^{0.5}$$

Uncertainty in Q_{in} is dominated by the uncertainty in the 2Ω resistance since voltage readings done by the acquisition system have a very low uncertainty.

$$\therefore \delta Q_{in}/Q_{in} = 0.03$$

For the chip chosen for calculations ;

$$\delta Q_{in} = (0.03)(0.351) = 0.01053 \text{ W}$$

Uncertainties for other variables are calculated as following :

$$\delta Q_{con}/Q_{con} = ((\delta(T_s - T_1)/(T_s - T_1))^2 + (\delta R_c/R_c)^2)^{0.5}$$

where

$$\delta(T_s - T_1) = ((\delta T_s)^2 + (\delta T_1)^2)^{0.5}$$

Uncertainty in net power ;

$$\delta Q_{conv} = ((\delta Q_{in})^2 + (\delta Q_{con})^2)^{0.5}$$

Uncertainty in h ;

$$\delta h/h = ((\delta Q_{conv}/Q_{conv})^2 + (\delta(T_{avg} - T_c)/(T_{avg} - T_c))^2)^{0.5}$$

Uncertainty in Nusselt number ;

$$\delta Nu/Nu = ((\delta h/h)^2 + (\delta k/k)^2 + (\delta L/L)^2)^{0.5}$$

$$= ((0.3047)^2 + (0.040)^2 + (10^{-5}/0.024)^2)^{0.5} = 0.3073.$$

Uncertainty in Rayleigh number is calculated the same method :

$$\delta Ra/Ra = ((\delta Gr/Gr)^2 + (\delta Pr/Pr)^2)^{0.5}$$

where

$$\delta Pr/Pr = ((\delta \nu/\nu)^2 + (\delta \alpha/\alpha)^2)^{0.5}$$

$$\therefore \delta Ra/Ra = 0.0284$$

APPENDIX C
PROGRAM LISTINGS

1. DATA ACQUISITION PROGRAM

```
10    !FILE NAME:THESIS1
20    !EDITED BY:TURGAY PAMUK,LTJG,TURKISH NAVY
30    !
40    !
50    !PROGRAM FOR GATHERING AND REDUCING DATA
60    !FOR 49 THERMOCOUPLES AND VOLTAGES FOR POWER
70    !SUPPLY.THERMOCOUPLES 1 TO 45 ARE ON THE
80    !BLOCKS.46 TO 49 ARE ON THE HEAT EXCHANGERS.
90    !
100   !
110   COM /Co/ D(7)
120   DIM Emf(59),Power(9),T(49)
130   !
140   !CORRELATION FACTORS TO CONVERT EMF TO DEGR-
150   !EES CELSIUS.
160   DATA 0.1008609,.2572,.9,-767345.8,78025936,
170   DATA -3247486589,6.38E9,-2.66E13,3.94E14
180   !
190   READ D(*)
200   Ro=2.000
210   PRINTER IS 701
220   BEEP
230   INPUT "ENTER THE INPUT MODE:0=SYS,1=FILE",Im
240   IF Im=1 THEN
250   BEEP
260   INPUT "ENTER NAME OF FILE",Oldfile$
270   PRINT USING "20X,""THESE RESULTS ARE FROM DATA FILE: "",10A":Oldfile$
280   BEEP
290   ELSE
300   BEEP
310   INPUT "ENTER NAME OF NEW DATA FILE",Newfile$
320   PRINT USING "20X,""DATA IS STORED IN DATA FILE : "",10A":Newfile$
330   BEEP
340   END IF
350   !
360   IF Im=1 THEN ASSIGN @File TO Oldfile$
370   IF Im=0 THEN
380   CREATE BDAT Newfile$,5
390   ASSIGN @File TO Newfile$
400   END IF
410   !
420   !NOW THE ACQUISITION SYSTEM WILL READ DATA
430   !
440   BEEP
450   BEEP
460   IF Im=0 THEN
470   OUTPUT 709;"AR AF00 AL58"
480   OUTPUT 722;"F1 R1 I1 Z1 FL1"
490   FOR I=0 TO 58
500   OUTPUT 709;"AS"
510   ENTER 722;Emf(I)
520   BEEP
530   NEXT I
540   OUTPUT @File;Emf(*)
550   ELSE
560   ENTER @File;Emf(*)
```

```
570   END IF
580   OUTPUT 709;"TD"
590   !CONVERSION FROM MVOLT TO CELCIUS
600   FOR I=0 TO 48
610   Sum=0.
620   FOR J=0 TO 7
630   Sum=Sum+D(J)*Emf(I)^J
640   NEXT J
650   T(I)=Sum
660   NEXT I
670   !
680   !POWER INPUT CALCULATION
690   J=1
700   Volt=Emf(49)
710   !
720   FOR I=50 TO 58
730   Pow(J)=Emf(I)*(Volt-Emf(I))/Rs
740   J=J+1
750   NEXT I
760   !
770   !
780   BEEP
790   BEEP
800   !PRINTS ALL THE COMPONENT TEMPERATURES AND POWERS
810   PRINT
820   PRINT
830   PRINT USING "20%,"" CENTER   TOP  RIGHT   LEFT BOTTOM    POWER(WATTS)"""
840   PRINT
850   PRINT
860   PRINT USING "12X,""CHIP NO1:"",5(3D.D,2X),4X,2D.DD,/":T(0),T(1),T(2),T(3),
T(4),Pow(1)
870   PRINT USING "12X,""CHIP NO2:"",5(3D.D,2X),4X,2D.DD,/":T(5),T(6),T(7),T(8),
T(9),Pow(2)
880   PRINT USING "12X,""CHIP NO3:"",5(3D.D,2X),4X,2D.DD,/":T(10),T(11),T(12),T(
13),T(14),Pow(3)
890   PRINT USING "12X,""CHIP NO4:"",5(3D.D,2X),4X,2D.DD,/":T(15),T(16),T(17),T(
18),T(19),Pow(4)
900   PRINT USING "12X,""CHIP NO5:"",5(3D.D,2X),4X,2D.DD,/":T(20),T(21),T(22),T(
23),T(24),Pow(5)
910   PRINT USING "12X,""CHIP NO6:"",5(3D.D,2X),4X,2D.DD,/":T(25),T(26),T(27),T(
28),T(29),Pow(6)
920   PRINT USING "12X,""CHIP NO7:"",5(3D.D,2X),4X,2D.DD,/":T(30),T(31),T(32),T(
33),T(34),Pow(7)
930   PRINT USING "12X,""CHIP NO8:"",5(3D.D,2X),4X,2D.DD,/":T(35),T(36),T(37),T(
38),T(39),Pow(8)
940   PRINT USING "12X,""CHIP NO9:"",5(3D.D,2X),4X,2D.DD,/":T(40),T(41),T(42),T(
43),T(44),Pow(9)
950   PRINT
960   PRINT
970   !
980   PRINT USING "5X,""HEAT EXCHANGER TEMPERATURES:   RIGHT  LEFT"""
990   PRINT USING "29X,""BOT:"",2X,2(3D.D,2X)":T(45),T(46)
1000  PRINT USING "29X,""TOP:"",2X,2(3D.D,2X)":T(47),T(48)
1010  BEEP
1020  !
1030  !
1040  PRINTER IS 1
1050  ASSIGN #File TO *
1060  END
```

2. HEAT TRANSFER CALCULATIONS PROGRAM

```
10    !FILE NAME:THESIS2
20    !EDITED BY:TURGAY PAMUK,LTJG,TURKISH NAVY
30    !
40    !
50    !PROGRAM TO ANALYZE THE RAW DATA IN THE DATA
60    !FILES OBTAINED FROM TEST RUNS
70    !
80    COM /Co/ D(7)
90    DIM Emf(59),Power(9),T(49),Tavg(9),Ts(9),Tfilm(9),Qnet(9),H(9),K(9),Rho(9)
,Cp(9),N(9),Nu(9)
100   DIM Ray(9),Delt(9),Alfa(9),Pr(9),Gr(9)
110   DIM Beta(9),Dpow(9),Dts(9),Dqloss(9)
120   !CORRELATION FACTORS TO CONVERT EMF TO DEGR-
130   !EES CELCIUS.
140   DATA 0.10086091,25727.9,-767345.8,78025596.
150   DATA -9247486589.6,98E+9,-2.66E13,3.94E14
160   !
170   READ D(*)
180   !RESISTANCE OF PRECISION RESISTOR : 3%
190   Rp=2.000
200   !PRINTER IS 701
210   BEEP
220   BEEP
230   INPUT "ENTER NAME OF FILE",Oldfile$
240   PRINT USING "20X,""THE RAW EMF DATA ARE FROM FILE: "",10A";Oldfile$
250   BEEP
260   BEEP
270   ASSIGN @File TO Oldfile$
280   ENTER @File;Emf(*)
290   !
300   FOR I=0 TO 48
310   Sum=0
320   FOR J=0 TO 7
330   Sum=Sum+D(J)*Emf(I)^J
340   NEXT J
350   T(I)=Sum
360   NEXT I
370   !
380   J=1
390   Volt=Emf(49)
400   FOR I=50 TO 58
410   Pow(J)=Emf(I)*(Volt-Emf(I))/Rp
420   Dpow(J)=.03*Pow(J)
430   !BECAUSE OF THE UNCERTAINTY IN RP
440   J=J+1
450   NEXT I
460   !
470   Acen=1.92E-4
480   Alef=1.44E-4
490   Arig=1.44E-4
500   Atop=4.8E-5
510   Abot=4.8E-5
520   Atot=5.76E-4
530   Tavg(1)=(T(0)*Acen+T(1)*Atop+T(2)*Arig+T(3)*Alef+T(4)*Abot)/Atot
540   Tavg(2)=(T(5)*Acen+T(6)*Atop+T(7)*Arig+T(8)*Alef+T(9)*Abot)/Atot
550   Tavg(3)=(T(10)*Acen+T(11)*Atop+T(12)*Arig+T(13)*Alef+T(14)*Abot)/Atot
560   Tavg(4)=(T(15)*Acen+T(16)*Atop+T(17)*Arig+T(18)*Alef+T(19)*Abot)/Atot
570   Tavg(5)=(T(20)*Acen+T(21)*Atop+T(22)*Arig+T(23)*Alef+T(24)*Abot)/Atot
580   Tavg(6)=(T(25)*Acen+T(26)*Atop+T(27)*Arig+T(28)*Alef+T(29)*Abot)/Atot
```

```
590   Tavg(7)=(T(30)*Acen+T(31)*Atop+T(32)*Arig+T(33)*Alef+T(34)*Abot)/Atot
600   Tavg(8)=(T(35)*Acen+T(36)*Atop+T(37)*Arig+T(38)*Alef+T(39)*Abot)/Atot
610   Tavg(9)=(T(40)*Acen+T(41)*Atop+T(42)*Arig+T(43)*Alef+T(44)*Abot)/Atot
620   !
630   !UNCERTAINTY OF TC READINGS
640   Dt=.2
650   Dtavg=((5*Dt^2)^.5)/5
660   Ta=20.
670   !UNCERTAINTY OF AMBIENT TEMPERATURE
680   Dta=1.
690   Totr=37.686
700   Dtotr=8.8324
710   Rc=54.979
720   Drc=23.225
730   Req=5.109
740   Dreq=.8620
750   !
760   !CHIP BACK SURFACE TEMPERATURES
770   FOR J=1 TO 9
780   Ts(J)=(Pow(J)/.083)+T((J-1)*5)
790   Tssum=Tssum+Ts(J)
800   Dts(J)=(145.159*Dpow(J)^2+Dt^2)^.5
810   Dtsavgsqr=Dtsavgsqr+Dts(J)^2
820   NEXT J
830   !
840   Tsavg=Tssum/9
850   Dtsavg=(Dtsavgsqr .5)/9
860   Qtotloss=(Tsavg-Ta)/Totr
870   Dqtot=Qtotloss*((Dtsavg^2+Dta^2)/(Tsavg-Ta)^2+(Dtotr/Totr)^2)^.5
880   T1=Qtotloss*(Totr-Req)+Ta
890   Dreif=(Dtotr^2+Dreq^2)^.5
900   Dmult=((Dqtot*(Totr-Req))^2+(Qtotloss*Dreif)^2)^.5
910   Dt1=(Dmult^2+Dta^2)^.5
920   !
930   !CONDUCTION LOSS CALCULATION
940   FOR J=1 TO 9
950   Qloss(J)=(Ts(J)-T1)/Rc
960   Dqloss(J)=Qloss(J)*((Dts(J)^2+Dt1^2)/(Ts(J)-T1)^2+(Drc/Rc)^2)^.5
970   NEXT J
980   !
990   !AVERAGE SINK TEMPERATURE CALCULATION
1000  Auo=4.32E-3
1010  Adown=4.32E-3
1020  Ain=2.448E-2
1030  !
1040  Tsink=(T(45)+T(46)+T(47)+T(48))/4
1050  Dtsink=((4*Dt^2)^.5)/4
1060  L=2.4E-2
1070  PRINT USING "2X,""QNET(W)      TAVG-TS      NU       %UNC.IN NU  RA*1.E-7  %U
NC.IN RA"",10A,/"
1080  !
1090  !
1100  !CALCULATION OF NET POWER,NU, RA AND UNCERTAINTIES
1110  FOR J=1 TO 9
1120  Qnet(J)=Pow(J)-Qloss(J)
1130  Dqnet=(Dpow(J)^2+Dqloss(J)^2)^.5
1140  Tfilm(J)=(Tavg(J)+Tsink)/2
1150  Dtfilm=((Dtsink^2+Dtavg^2)^.5)/2
1160  Delt(J)=Tavg(J)-Tsink
1170  Ddelt=2*Dtfilm
```

```
1180  H(J)=Qnet(J)/(Atot*Delt(J))
1190  Dn=H(J)*((Dqnet/Qnet(J))^2+(Ddelt/Delt(J))^22)^.5
1200  K(J)=.65-7.89474E-4*Tfilm(J)
1210  Dk=7.8947E-5*Dtfilm
1220  K(J)=K(J)/10.
1230  Rho(J)=1.825-.00246*Tfilm(J)
1240  Drho=1000.*.00246*Dtfilm
1250  Rho(J)=Rho(J)*1000.
1260  Cp(J)=.241111+(3.7037E-4)*Tfilm(J)
1270  Dcp=4180.*3.7037E-4*Dtfilm
1280  Cp(J)=Cp(J)*4180.
1290  N(J)=1.4074-2.964E-2*Tfilm(J)+3.8018E-4*Tfilm(J)^2-2.7308E-6*Tfilm(J)^3+8.
1679E-9*Tfilm(J)^4
1300  Dn=Dtfilm*(8.785E-4+(7.604E-4*Tfilm(J))+(2.458E-6*Tfilm(J)^2)^2+(2.45E-8*T
film(J)^3)^2)^.5
1310  Dn=Dn*1.E-6
1320  N(J)=N(J)*(1.E-6)
1330  Beta(J)=.00245/(1.825-.00246*Tfilm(J))
1340  Alfa(J)=K(J)/(Rho(J)*Cp(J))
1350  Dalfa=Alfa(J)*((Dk/K(J))^2+(Drho/Rho(J))^2+(Dcp/Cp(J))^2)^.5
1360  Pr(J)=N(J)/Alfa(J)
1370  Dpr=Pr(J)*((Dn/N(J))^2+(Dalfa/Alfa(J))^2)^.5
1380  Nu(J)=H(J)*L/K(J)
1390  Dnu=Nu(J)*((Dh/H(J))^2+(Dk/K(J))^2)^.5
1400  Pernu=(Dnu/Nu(J))*100.
1410  Gr(J)=9.81*Beta(J)*(L^3)*Delt(J)/N(J)^2
1420  Dgr=Gr(J)*((Ddelt/Delt(J))^2+(2*Dn/N(J))^2)^.5
1430  Ray(J)=Gr(J)*Pr(J)
1440  Dray=Ray(J)*((Dgr/Gr(J))^2+(Dpr/Pr(J))^2)^.5
1450  Perray=(Dray/Ray(J))*100.
1460  Ray(J)=Ray(J)/1.E+7
1470  PRINT USING "2X,2D.DDD,5(6X,2D.DD),/";Qnet(J),Delt(J),Nu(J),Pernu,Ray(J),
Perray
1480  NEXT J
1490  !ASSIGN *File TO *
1500  END
```

LIST OF REFERENCES

1. Chu, R.C., *"Heat Transfer in Electronic Systems"*, Hemisphere Publisher Inc., Heat Transfer 1986, v.6, pp. 293-306.

2. Knock, R.H., *"Flow Visualiation Study of Natural Convection from A Heated Protrusion in a Liquid Filled Enclosure"*, Master's Thesis, Naval Postgraduate School, Dec. 1983.

3. Kohara, K. Nakao, S. Tsutsumi, K. Shibata, H. and Nakata, H., *"High Thermal Conduction Package Technology for Flip Chip Devices"*, IEEE Transactions on Components, Hybrids and Manufacturing Technology, v.6, no.3, Sep. 1983.

4. Kishimoto, T. Sasaki, E. and Moriya, K., *"Gas Cooling Enhancement Technology for Integrated Circuit Chips"*, IEEE Transactions on Components, Hybrids and Manufacturing Technology, v.7, no.3, Sep. 1984.

5. Kraus, A. D., *"Thermal Analysis and Control of Electronic Equipment"*, Hemisphere Publisher Inc., pp.377-407, 1983.

6. Bar-Cohen, A. *"Thermal Design of Immersion Cooling Modules for Electronic Components"*, Heat Transfer Engineering, v.4, nos. 3-4, Jul.-Dec. 1983.

7. Liu, K.V., Yang,K.T., and Kelleher,M.D., *"Three Dimensional Natural Convection Cooling of an Array of Heated Protrusions in an Enclosure Filled with a Dielectric Fluid"* Proceedings of International Symposium on Cooling Tecnhology of Electronic Equipment, March 17-21 1987, pp. 486-497, 1987.

8. Acharya, S. and Goldstein, R.J., *"Natural Convection in an Externally Heated Vertical or Inclined Square Box Containing Internal Energy Sources"*, Journal of Heat Transfer, November 16, 1983.

9. Torok, D., *"Augmenting Experimental Methods for Flow Visualization and Thermal Perfomance Prediction in Electronic Packaging Using Finite Elements"*, 22nd national heat transfer conference and exhibition, August 5-8 1984, ASME HTD v.32, pp. 49-57, 1984.

10. Kuhn, D. and Oosthuizen, P.H., *"Three Dimensional Transient Natural Convective Flow in a Rectangular Enclosure With Localized Heating"*, Winter Annual Meeting of ASME, 12-17 December 1986, ASME HTD v.63, pp. 55-62, 1986.

11. Shakerin, S., Bohn, M. and Loehrke, R.I., *"Natural Convection in an Enclosure with Discrete Roughness Elements on a Vertical Heated Wall"*, Proceedings of International Heat Transfer Conference, 17-22 August 1986, v.4, pp. 1519-1525, 1986.

12. Liu, K.V., Yang, K.T., Wu, Y.W. and Kelleher, M.D., *"Local Oscillatory Surface Temperature Responces in Immersion Cooling of a Chip Array by Natural Convection in an Enclosure"* Proceedings of the Symposium on Heat and Mass Transfer, October 1-2 1987, pp. 309-330, 1987

13. Park, K.-A. and Bergles, A.E., *"Natural Convection Heat Transfer Characteristics of Simulated Microelectronic Chips"*, Journal of Heat Transfer, v.109, pp. 90-96, Feb. 1987.

14. Filis, P. and Poulikakos, D., *"An Experimental Study of the Effect of Wall Nonuniformity on Natural Convection in an Enclosure Heated from the Side"*, Int. J. Heat and Fluid Flow, v.7, no. 4, pp. 258-265, Dec. 1986.

15. Anderson, R. and Bohn, M., *"Heat Transfer Enhancement in Natural Convection Enclosure Flow"*, Winter Annual Meeting of ASME, 9-14 December 1984 Journal of Heat Transfer, v.108, no. 2, pp.330-336, May 1986.

16. Yang, R. and Yao.L.S., *"Natural Convection Along a Finite Vertical Plate"*, Journal of Heat Transfer, v.109, pp. 363-413, May 1987.

17. Beckermann, C., Ramadhyani, S. and Viskanta, R, *"Natural Convection Flow and Heat Transfer Between a Fluid Layer and a Porous Layer Inside a Rectangular Enclosure"*, Journal of Heat Transfer, v.109, pp. 363-413, May 1987.

18. Kulkarni, A.K., Jacobs, H.R. and Hwang, J.J., *"Similarity Solution for Natural Convection Flow over an Isothermal Vertical Wall Immersed in Thermally Stratified medium"*, Int. J. Heat Mass Transfer, v.30, no. 4, pp. 691-698, 1987.

19. Lankford, K.E. and Bejan, A., *"Natural Convection in a Vertical Enclosure Filled With Water near 4 °C"*, Journal of Heat Transfer, v.108, pp. 755-763, Nov. 1986.

20. Bohn, M.S. and Kirkpatrick, A.T., *"High Rayleigh Number Natural Convection in an Enclosure Heated from Below and From the Sides"*, Natural Heat Transfer Conference, 24-28 July 1983 ASME HTD, v.26, pp. 27-33, 1983.

21. Kline, S.J.and McClintock, F.A., *"Describing Uncertainties in Single-sample Experiments"*, Mechanical Engineering , p.3, Jan. 1953.

22. Holman, J.P., *"Heat Transfer"*, Mc-Graw Hill, pp. 265-305, 1981.

23. Kays., W.M. and Crawford., M.E., *"Convective Heat and Mass Transfer"* , Mc-Graw Hill, pp. 313-331, 1980.

INITIAL DISTRIBUTION LIST

		No. Copies
1.	Defense Technical Information Center Cameron Station Alexandria, VA 22304-6145	2
2.	Library, Code 0142 Naval Postgraduate School Monterey, CA 93943-5002	2
3.	Professor M. D. Kelleher, Code 69KK Department of Mechanical Engineering Naval Postgraduate School Monterey, CA 93943	2
4.	Professor Y. Joshi, Code 69JI Department of Mechanical Engineering Naval Postgraduate School Monterey, CA 93943	1
5.	Department Chairman Code 69 Department of Mechanical Engineering Naval Postgraduate School Monterey, CA 93943	1
6.	Deniz Kuvvetleri K.ligi Personel ve Egitim Daire Baskanligi Bakanliklar/ANKARA-Turkey	4
7.	Istanbul Technical University Makina Muhendisligi Fakultesi Isi Transferi Kursusu Macka/ISTANBUL-Turkey	1
8.	Bosphorus University Makina Muhendisligi Fakultesi Isi Transferi Kursusu ISTANBUL-Turkey	1
9.	Middle East Technical University Makina Muhendisligi Fakultesi Isi Transferi Kursusu ANKARA-Turkey	1
10.	Turgay Pamuk Ogretmenler Sitesi Odul Sok., A Blok, No=11 Ambarli/ISTANBUL-Turkey	1

Thesis
P14533
c.1

Pamuk
Natural convection immersion cooling of an array of simulated chips in an enclosure filled with dielectric liquid.